DEVELOPMENT OF Mn/TiO$_2$ PHOTOCATALYST FOR HYDROGEN PRODUCTION FROM WATER UNDER VISIBLE LIGHT

by

Syarifah Nor Faizah bt Syed Abdul Rahman

Dissertation submitted in partial fulfillment of

the requirements for the

Bachelor of Engineering (Hons)

(Chemical Engineering)

JULY 2010

Universiti Teknologi PETRONAS

Bandar Seri Iskandar

31750 Tronoh

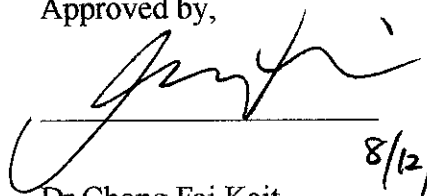Perak Darul Ridzuan

CERTIFICATION OF APPROVAL

DEVELOPMENT OF Mn/TiO$_2$ PHOTOCATALYST FOR HYDROGEN PRODUCTION FROM WATER UNDER VISIBLE LIGHT

by

Syarifah Nor Faizah bt Syed Abdul Rahman

A project dissertation submitted to the

Chemical Engineering Programme

Universiti Teknologi PETRONAS

in partial fulfilment of the requirement for the

BACHELOR OF ENGINEERING (Hons)

(CHEMICAL ENGINEERING)

Approved by,

_____   8/12/10

Dr Chong Fai Kait

Project Supervisor

Assoc. Prof. Dr Chong Fai Kait
Fundamental & Applied ... Department
Universiti ...
... Seri Iskandar, ...
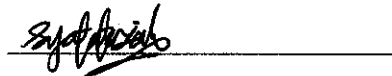Perak Darul Ridzuan, MALAYSIA

UNIVERSITI TEKNOLOGI PETRONAS

TRONOH, PERAK

JULY 2010

CERTIFICATION OF ORIGINALITY

This is to certify that I am responsible for the work submitted in this project, that the original work is my own except as specified in the references and acknowledgements, and that the original work contained herein have not been undertaken or done by unspecified sources or persons.

SYARIFAH NOR FAIZAH BT SYED ABDUL RAHMAN

ABSTRACT

TiO$_2$ photocatalyst doped with manganese are prepared by wet impregnation methods. By doping TiO$_2$ with manganese, hydrogen can be produced with photocatalytic decomposition of water under visible light irradiation. Manganese(II) nitrate has been used to prepare manganese doped catalyst via wet impregnation. In order to find the best calcination temperature, three calcination temperature are selected; 300 $^{\circ}$C, 400 $^{\circ}$C and 500 $^{\circ}$C. The samples were characterized by thermogravimetric analysis (TGA), diffuse reflectance UV-Vis (DR-UV-Vis), Field emission-Scanning electron microscopy (FE-SEM), Fourier transform infrared (FTIR) spectroscopy and X-ray diffraction (XRD). Doping TiO$_2$ with manganese metal reduce the energy levels for the band gap of TiO$_2$, shifting activity from UV region (wavelength, λ < 400 nm) to visible light region. It was found that 5 wt% Mn/TiO$_2$ calcined at 400 $^{\circ}$C produced the maximum amount of hydrogen (6.3 mL in distilled water and 6.6 mL in sea water). The reduction in band gap energy was estimated from transformed of Kubelka-Munk plot. The estimated band gap energy for 5Mn_4 was 2.95. The influence of the process parameters on catalytic activity is also explained.

ACKNOWLEDGEMENT

First of all, I would like to praise Allah the Almighty, who has been guiding, helping and giving me the strength to complete my Final Year Project.

My utmost gratitude goes to my supervisor, Dr. Chong Fai Kait for her most valuable guidance, support and constructive criticism throughout the project. I am really appreciate her effort in providing me a great supervision in order to let this project achieves its objectives and complete in two semesters.

My sincere thanks to Chemical Engineering Department of Universiti Teknologi PETRONAS (UTP) for providing all the facilities needed throughout the project. Here, I would like to express my full appreciation to Ms Ela and Ms Nadia who have shared their knowledge and provided the necessary guidance throughout the project, lab technologist and also Mechanical Engineering Department for their willingness in providing the full support and cooperation when I am in need.

Last but not least, I also would like to seize this opportunity to thank to my parents, family members and friends who are providing me with encouragement in completing this Final Year Project. Those directly and indirectly support, guidance and encouragement from all parties will always be an unforgettable memory throughout my life and it would be very useful in the future.

TABLE OF CONTENTS

LIST OF FIGURES

LIST OF TABLES

CHAPTER 1 : INTRODUCTION

1.1 Background of Study

In this day and age, energy supply system, electricity, diesel fuel and natural gases are used as energy carriers. Utilization of all these energy carriers may lead to global warming issues. Even in industries nowadays, hydrogen has been primarily used as a reactant. Thus, hydrogen has been studied and identified as the future energy carrier. The reasons why hydrogen becomes the most preferred energy carrier for the future is because it i) has high efficiency ii) can be produced safely from renewable energy sources iii) can be used as a fuel for "zero emissions" vehicles, heating purposes and power generations

It is found that by using hydrogen in transportation sector, the performance of the vehicles will be increased and the pollution can be reduced. Based in the secondary energy infobook done by National Energy Education Development Project, by adding around 5% hydrogen to gasoline can reduce 30 to 40 percent emissions of nitrogen oxide in today's engine where an engine will burn pure hydrogen producing only water and minute amount of nitrogen oxide as exhaust (2010). Hydrogen cannot be found directly on earth, thus, it must be manufactured.

Today, almost all hydrogen is produced via steam reforming of natural gas at oil refineries. Hydrogen is separated from methane (CH_4) by reacting with steam at high temperature. This hydrogen is used for industrial purposes. This steam reforming method gives effect to the environment where "greenhouse gas" which is CO_2 is also produced during hydrogen generation. According to Guido Collodi and Foster Wheeler, with this method, 9 to 12 tons CO_2 is produced for a ton of H_2 produced (Collodi & Wheeler, 2009). The reaction is shown below:

$$CH_4(g) + 2H_2O(g) \leftrightarrow CO_2(g) + 4H_2(g)$$
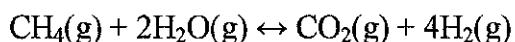
The reaction above is divided into 2 steps where in the first step methane reacts with water vapour (steam) and in the second step carbon monoxide produced from the first step reacts with steam.

$$CH_4 + H_2O \leftrightarrow CO + 3H_2$$

$$CO + H_2O \leftrightarrow CO_2 + H_2$$
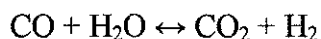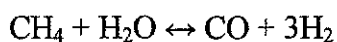
This situation will lead to global warming issue. However, the environmental issue can be solved by finding ways to produce hydrogen gas by using energy sources that is renewable, for example, radiation from light which is "free" and abundance. It can also avoid the emissions of greenhouse gases due to hydrogen production from fossil fuel; thus, solve the environmental and energy problems related to hydrogen production.

Recently, there are many research have been done in producing hydrogen gas from renewable energy. Photoreduction of water process is an alternative way in order to produce hydrogen. In this process, hydrogen will be produced from water in the presence of light. For this purpose, TiO_2 become the most preferred material to act as photocatalsyt (Dholam *et al.*, 2009). Catalyst is a substance that increases the rate of a chemical reaction. This is done by reducing the activation energy, but at the same time does not change the reaction.
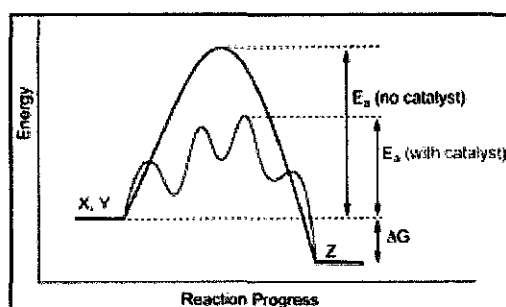
Figure 1.1: Activation Energy with and without catalyst.
(http://en.wikipedia.org/wiki/File:CatalysisScheme.png)

Photocatalyst is a catalyst that accelerates photoreaction. It is activated by light and the photocatalytic activity (PCA) depends on the ability of the catalyst to create electron–hole pairs.

Once the photocatalyst receive the energy from light, it will be transformed into high energy state material. Electrons which is located at "valence band" will jump to "conduction band" if the energy received is high enough (Brezova *et al.*, 1997). This situation can be illustrated in the Figure 1.2. The application of

2

photocatalyst can be seen in the study of photocatalytic water splitting process for hydrogen production.
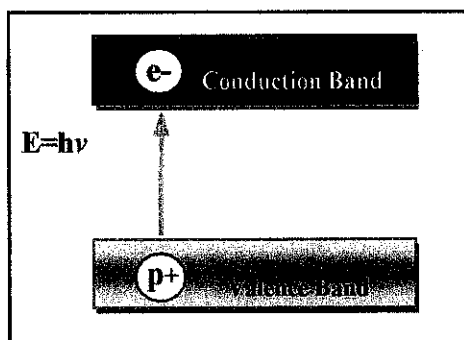
Figure 1.2: Illustration of electron receiving energy from light.

Using TiO_2 photocatalyst alone needs UV light and not visible light in order to produce hydrogen. Doping TiO_2 catalyst with metal can lead to hydrogen production under irradiation of visible region of sunlight. Many metals have been studied to overcome this problem and the most preferred transition metals studied are Cu, Fe and Cr (Bae *et al*, 2007; Brezova *et al.*, 1997; Choi *et al.*, 1994; Dholam *et al.*, 2009; Dvoranova *et al*, 2002; Zhang *et al*, 2004).

Among all the transition metals, manganese as photocatalyst is the least studied metal for hydrogen production. This manganese is said to be a good reduction and oxidation agent (Liu *et al.*, 2001; Sreekanth *et al.* 2008; Wu *et al.*, 2007; Xin *et al.*, 2004). Thus, manganese has been chosen to be explored in this project to develop visible light-active Mn/TiO_2 photocatalyst for H_2 production from water.

In order to understand more in this photocatalyst area, literature review on background of TiO_2 photocatalyst and the reason why manganese metal is chosen as metal doped on TiO_2 is summarized in Chapter 2. Studies and discoveries that have been done before regarding doping TiO_2 with transition metal such as copper and iron also included in this chapter.

In this project, a series of Mn/TiO_2 photocatalysts are synthesized using wet impregnation method. The catalysts are characterized using thermogravimetric analysis (TGA) , diffuse reflectance UV-Vis (DR-UV-Vis, field emission-scanning

electron microscopy (FE-SEM) , Fourier transform infrared (FTIR) spectroscopy and X-ray diffraction (XRD) . The details of the methodology are discussed in Chapter 3.

All the results obtained are reported in chapter 4. In order to choose the best calcination temperature and metal loading for Mn/TiO_2 photocatalyst, the comparison between samples are done. The best photocatalyst will be determined by comparing how much hydrogen produced during the reaction. In this project, the best photocatalyst is the one that produce the highest amount of hydrogen after 2h reaction. Characteristics of the best and the worst photocatalyst also discussed here. The whole project will be concluded in the last chapter which is chapter 5.

1.2   Problem Statement

Producing hydrogen through photocatalytic reaction can be conducted by the photoreduction process of water. This method utilizes solar energy to produce hydrogen and material used for the photocatalyst is titanium dioxide, TiO_2. TiO_2 alone will mostly absorb the ultraviolet portion of the solar spectrum. It is not an economically feasible option if UV radiation is required for photocatalytic reaction. Thus, shifting the active region of the photocatalyst from UV region to visible region of sunlight is needed and very relevant since the source is "free" and in abundance. This could be accomplished by doping TiO_2 with transition metals.

1.3   Objective and Scope of Study

The objective of this project is to develop visible light-active Mn/TiO_2 photocatalyst by using wet impregnation method for H_2 production from water. The scope of study includes doping TiO_2 with transition metal; manganese, determining the photocatalyst performance under visible light, determining the best the calcination temperature and characterizing the photocatalyst.

4

CHAPTER 2 : LITERATURE REVIEW

2.1   Titanium Dioxide, TiO_2

Photoreduction of water process is an alternative way of hydrogen generation. In this process, hydrogen will be produced from water in the presence of light. Titanium dioxide, TiO_2 has been considered the most active photocatalyst (Sreethawong *et al.*, 2009; Yoong *et al.*, 2009). Titanium dioxide is a naturally occurring oxide of the element titanium. It is also known as titania. This semiconducting oxide TiO_2 has been chosen because of its physically and chemically stable, strong oxidizing power, ease of availability, electronic properties (can be vary by changing the lattice defect chemistry or the oxygen stoichiometry), friendly to environment, high resistance to corrosion, non-toxicity and cheap (Dholam *et al.*, 2009; Li *et al.*, 2007; Liu *et al.*, 2006). Besides that, it is reported that it has been considered the most active photocatalyst because of its comparatively high photocatalytic efficiency (Sreethawong et al., 2009).

Even with all these advantages, titania has some disadvantages. TiO_2 photocatalyst has high band gap energy which is around 3.2 eV (Bae *et al.*, 2007; Dvoranova *et al.*, 2002; Yoong *et al.*, 2009). With this high energy band gap, TiO_2 alone can only absorb near-UV range which having wavelength, $\lambda < 400nm$ (Bae *et al.*, 2007; Dvoranova *et al.*, 2002; Yoong *et al.*, 2009). Thus, hydrogen gases only can be produced under UV light which is not an economically feasible. In order to overcome this problem, the absorption edge of TiO_2 must be shifted from UV light region to visible light region where the application of this TiO_2 photocatalyst can be done with involving direct sunlight. Thus, the chemical structure of TiO_2 needs to be modified.

ion, cobalt ion and manganese ion in the titania structure caused significant absorption shift from UV region into visible region compared to titania alone (Dvoranova et al., 2002). It is found that TiO_2 nanotubes need to be promoted with Pt metal to enhance its photocatalytic activity for producing hydrogen gas from neat ethanol (Lin et al., 2004). Based on Lin et al., higher Pt loading on TiO_2 nanotubes resulted in more stable catalyst that produced more H_2 (2004).

In a nutshell, the activity of photocatalyst can be increased by doping TiO_2 photocatalyst with transition metal ion. By doing so, the absorption edge of titania can be shifted from UV region.

2.3 Mn-doped TiO_2

A lot of transition metals have been explored in order to shift the absorption edge of TiO_2 into visible region for hydrogen production. Mn doping is very rare in the study and has been less explored compared to other transition metal such as Fe, Cu, Cr, Ni and Zn. Mn is known as a good oxidation and reduction agent. By doping Mn metal into TiO_2, the absorption edge also can be shifted from UV light region to visible light region (Zhang et al., 2004). Liu et al. researched on catalytic oxidation of chlorobenzene on supported manganese oxide catalyst (Liu et al., 2001). He reported that titania supported catalyst (MnO_x/TiO_2) displayed the highest catalytic activity and stability. The catalyst activity can be stable for over 82 hours except for the first 10 hours (Figure 2.1).
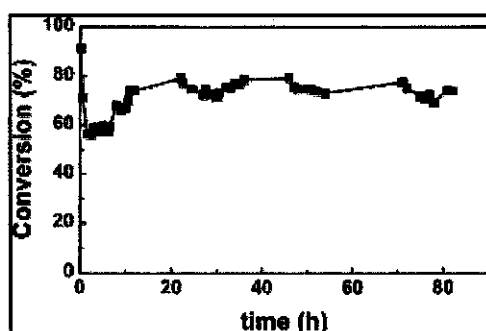

Figure 2.1: Catalytic activities as a function of time for chlorobenzene oxidation on MnO_x/TiO_2 catalyst
(Liu et al., 2001).

7

Zhang *et al.* did a study on the optical properties of Mn-doped TiO_2 thin films (2004). Based on the study, there is a gradual shift of the emission peak towards longer wavelength region (Figure 2.2) and a decrease in the peak intensity [30]. This is showing that the band gap energy of TiO_2 has been lowered by doping TiO_2 photocatalyst with Mn metal.

Xin *et al.* have conducted study on the effect of various transition metals (Cr, Mn, Fe, Co, Ni) for acetic acid photocatalytic degradation and carbon dioxide photocatalytic reduction in aqueous suspension, used as probe reaction (2004). It is reported that at 0.2M concentration of acetic acid, Mn/TiO_2 displayed the highest degradation rate. Mn can also be used as reducing agent for low temperature selective catalytic reduction of NO to NH_3 (Wu *et al.*, 2007). Sreekanth *et al.* (2008) compared Mn/TiO_2 catalyst with other doped TiO_2 catalyst for reduction of NO. The result showed that at 200 °C reaction, Mn/TiO_2 displayed the best catalytic activity for reduction of NO with CO compared to Ni/TiO_2, Cu/TiO_2, Cr/TiO_2 and Fe/TiO_2 (Figure 2.3).
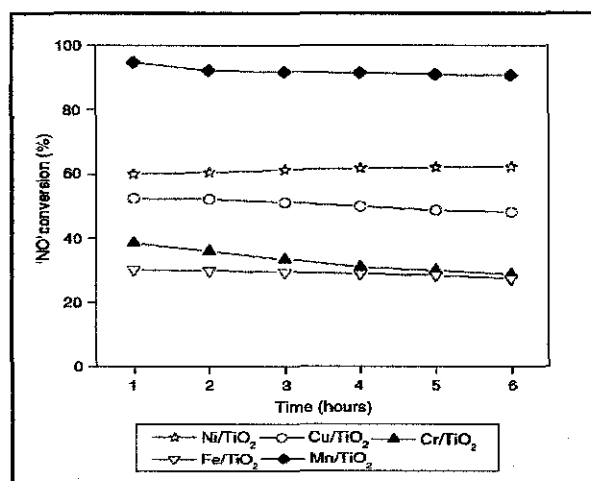
Figure 2.2: Catalytic activity of various titania supported catalyst at 200 °C for reduction of NO with CO. (Sreekanth *et al.*, 2008).

Based on previous studies discussed, Mn-doped TiO_2 is a good oxidation and reduction agent, thus, it is believed to have high potential to be doped onto TiO_2 photocatalyst to produce hydrogen gases under visible light. This Mn-doped TiO_2 photocatalyst is prepared via wet impregnation (Hu *et al.*, 2008).

CHAPTER 3 : METHODOLOGY

The scope of work is divided into 3 parts which is:

- ➤ Preparation and pre-treatment of photocatalyst
- ➤ Photocatalytic activity (reaction)
- ➤ Characterization of the photocatalysts

3.1   Chemicals and Equipments

For this project, there are chemicals needed for photocatalyst preparation and pre-treatment:

- ➤ TiO_2 (Degussa P25)
- ➤ Manganese(II) nitrate, $Mn(NO_3).6H_2O$ (Systerm)

The major equipments that will be used during this project are listed below:

- ➤ Thermogravimetric analysis (TGA)
- ➤ Diffuse reflectance UV-Vis (DR-UV-Vis)
- ➤ Field emission -Scanning electron microscopy (FE-SEM)
- ➤ Fourier transform infrared (FTIR) spectroscopy
- ➤ X-ray diffraction (XRD)
- ➤ Multiport reactor
- ➤ Oven
- ➤ Furnace

3.2   Photocatalyst Preparation

Photocatalyst were synthesized by wet impregnation method. TiO_2 powder (Degussa P25) was added into manganese(II) nitrate aqueous solution and stirred for 1 hour, forming a suspension. The solvent was then evaporated in a water bath at 80 °C until it became dense. The mixture was dried in an oven at 120 °C overnight (Hu *et al.*, 2008). Finally, calcination was conducted at 300 °C, 400 °C and 500 °C for 30 minutes. The process flow for Mn/TiO_2 preparation is shown in Figure 3.1. The photocatalyst prepared are given notation in the form of xMn_y where x is the wt% of Mn loading, Mn refers to Mn/TiO_2 and y refers to calcination temperature (x100 °C). Table 3.1 provides the summary of photocatalysts prepared.

```
┌─────────────────────────────────────────────────────┐
│   Mn(NO₃)₂ solution + TiO₂ powder (Degussa P25)      │
└─────────────────────────────────────────────────────┘
                        │ Stir 1 hour
                        ▼
┌─────────────────────────────────────────────────────┐
│                    Suspension                        │
└─────────────────────────────────────────────────────┘
                        │ Evaporation at 80 °C
                        │ Drying at 120 °C
                        ▼
┌─────────────────────────────────────────────────────┐
│                 Raw photocatalyst                    │
└─────────────────────────────────────────────────────┘
                        │ Calcination at 300 °C,
                        │ 400 °C and 500 °C
                        ▼
┌─────────────────────────────────────────────────────┐
│                   Photocatalyst                      │
└─────────────────────────────────────────────────────┘
```
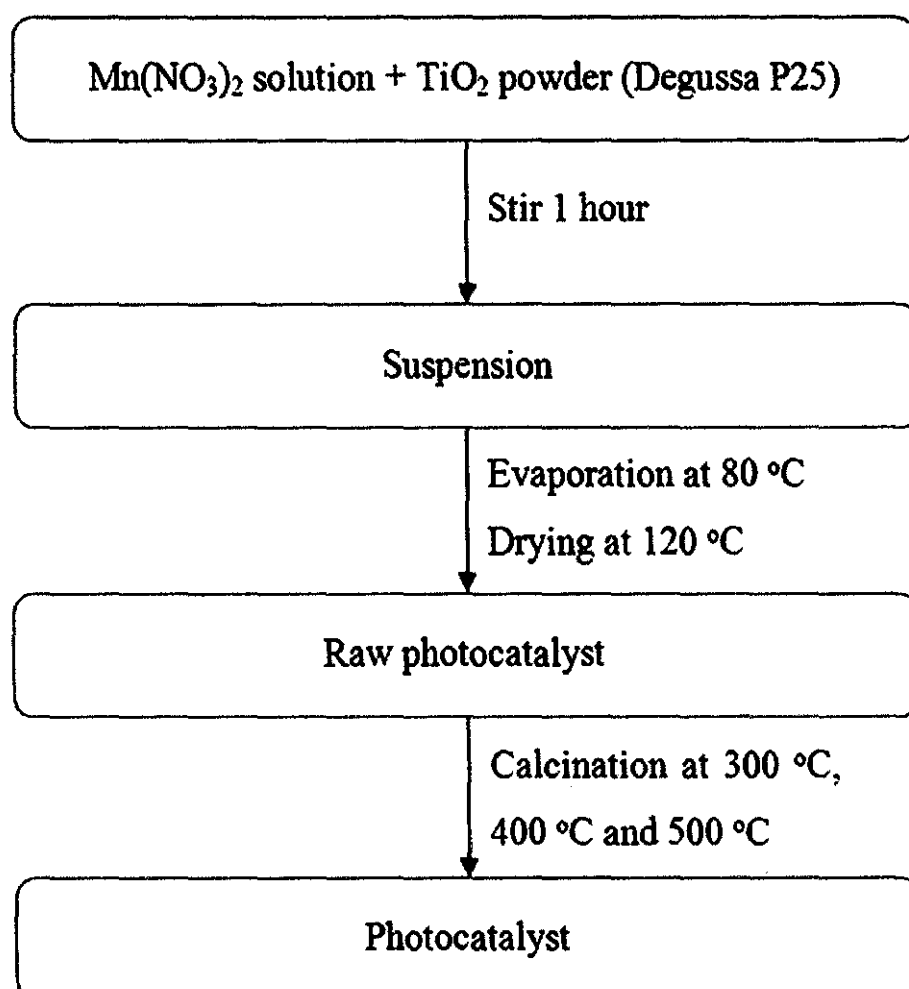
Figure 3.1: Steps to prepare Mn/TiO_2 photocatalyst.

Table 3.1: Summary of photocatalyst prepared calcined at different temperature for 30 minutes.

Mn loading (wt%)	Calcination temperature (^{o}C)		
	300	400	500
1	1Mn_3	1Mn_4	1Mn_5
5	5Mn_3	5Mn_4	5Mn_5
10	10Mn_3	10Mn_4	10Mn_5

3.3   Photocatalytic Activity

This study was performed at room temperature which is around 23°C by using a multiport photocatalytic reactor. To simulate the visible light, 500W halogen lamp is used. The lamp was fixed at a position 13 cm above the multiport reactor. The catalyst (0.1 g) was then dispersed in 8 mL distilled water. By using vertical graduated glass tube, the amount of gas evolved is monitored every 10 minutes for 2h.

3.4   Catalyst Characterization

3.4.1   Fourier Transform Infrared Spectroscopy (FTIR)

1 mg of catalyst with 200 mg of IR-grade KBr were ground and pressed into a pellet by using a hydraulic press. The FTIR spectrum of the sample, taken over a wave-number range of 450 cm^{-1} – 4000 cm^{-1}, is recorded as the percentage of transmittance (%T) versus wave-number. This FTIR analysis is useful for determining the functional groups present in the catalyst before and after the calcination. These functional groups can be identified by characteristic peaks on the spectrum.

3.4.2 Diffuse Reflectance Spectroscopy (DR-UV-Vis)

Diffuse reflectance UV-Vis spectra are recorded using a Perkin Elmer Lambda 900 instrument with an integrating sphere attachment using $BaSO_4$ powder as an internal reference. A layer of sufficiently thick powder sample (1 mm-3 mm) need to be prepared in order to ensure all the incident light will be absorbed or scattered before reaching the back surface of the sample holder. The result will be plotted as Kubelka-Munk function vs. wavelength. The indication of the absorption edge has been shifted to visible region or not can be determined through the relative position of the catalyst absorption edge compared to TiO_2 in the diffuse reflectance spectra. The band gaps (E_g) for all catalysts can be determined from extrapolation of the linear fit to the Tauc plot onto the photon energy axis. The illustration of Tauc plot is shown in the Figure 3.3.
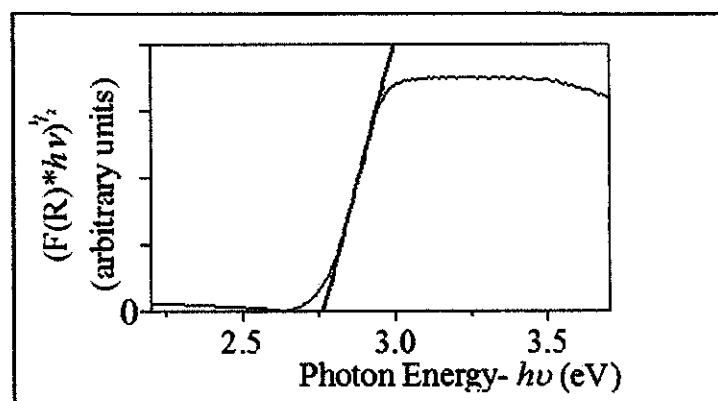

Figure 3.2: Illustration of Tauc plot. (retrieved from:
http://www.msm.cam.ac.uk/ascg/characterisation/uvvis.php)

3.4.3 Field Emission Scanning Electron Microscopy (FE-SEM)

The catalyst morphologies are determined by using FE-SEM. The samples are coated with platinum-palladium prior scanning at 100K magnification. From the FE-SEM micrographs, how well the dopant material is dispersed on the base material, TiO_2, in a catalyst sample can be seen.

3.4.4 X-ray Diffusion (XRD)

In order to identify the type of Mn species and also TiO_2 phase present on the photocatalyst, powder-XRD is conducted on the catalyst with $MnK\alpha$ radiation of 40 kV, 40 mA; 2θ angles from 10° up to 80° and scan speed of $4^{\circ}/min$. In order to determine the species present in a sample, XRD peaks are compared to the standards.

3.4.5 Thermogravimetric Analysis (TGA)

In order to determine the thermal stability of the catalyst due to calcinations process, this analysis has been carried out. Heating rate was maintained at 20 °C/min and the air flowing was set to 20 mL/min. The measurement was carried out with 30 °C to 850 °C temperature range.

CHAPTER 4 : RESULTS

4.1 Photocatalytic Activity

The activities of the photocatalysts were determined by investigating them in terms of Mn metal loading and calcination temperature. The amount of hydrogen gases produced for 2 hours reaction in distilled water for all photocatalyst samples were displayed in Figure 4.1. For 5 wt% Mn/TiO$_2$, the amount of hydrogen gases evolved increase 4.9 mL to 6.3 mL (29.18%) when the calcinations temperature was increased from 300 °C to 400 °C. However, the amount of hydrogen gases evolved decrease to 3.6 mL (42.65%) when the calcinations temperature was increased to 500 °C. The best activity is displayed by 5Mn_4 as it produces the highest amount of hydrogen gases which is 6.3 mL. Pure titania only produced 2.4 mL hydrogen.
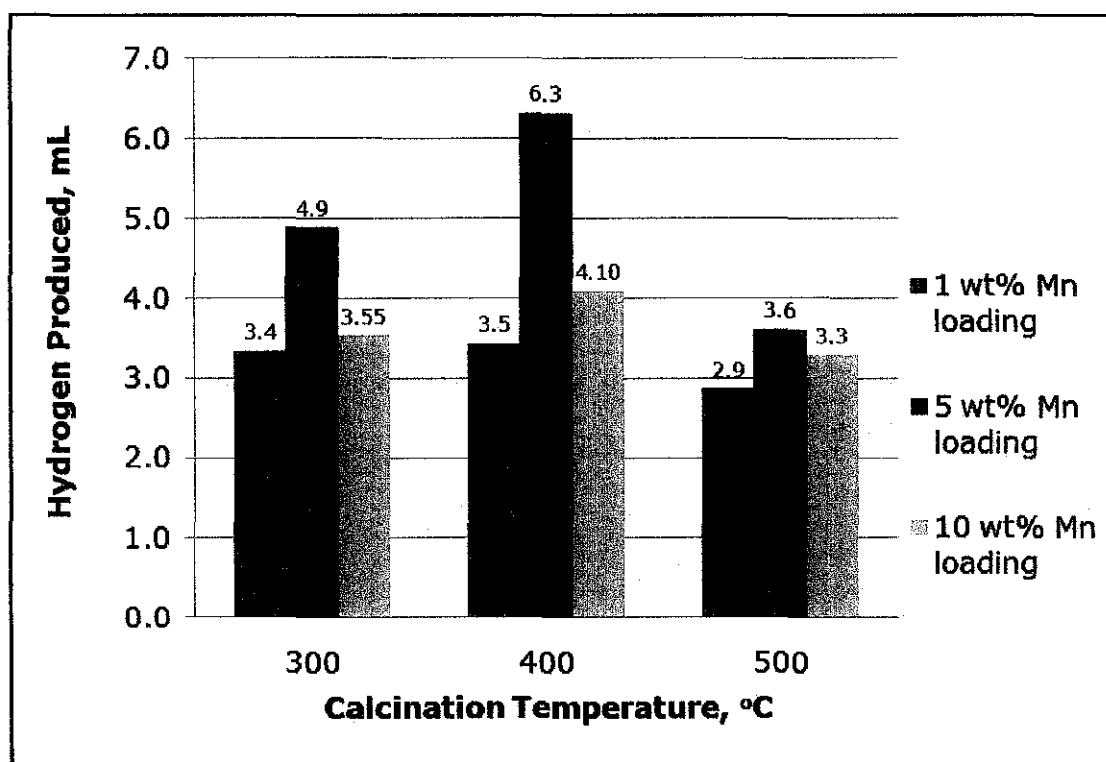
Figure 4.1: The effect of calcination temperature and metal loading on H$_2$ production.

Overall, 5 wt% Mn/TiO$_2$ photocatalyst showed the best photocatalytic activities for all the three different calcination temperatures (300 °C, 400 °C and 500 °C). The comparison between the photocatalysts' performance is displayed in Figure 4.2. From the results obtained, it is shown that for the first 50 minutes, there was not

much difference between those three samples. However, after 50 minutes reaction 5Mn_4 showed the best activity followed by 5Mn_3 and finally 5Mn_5.
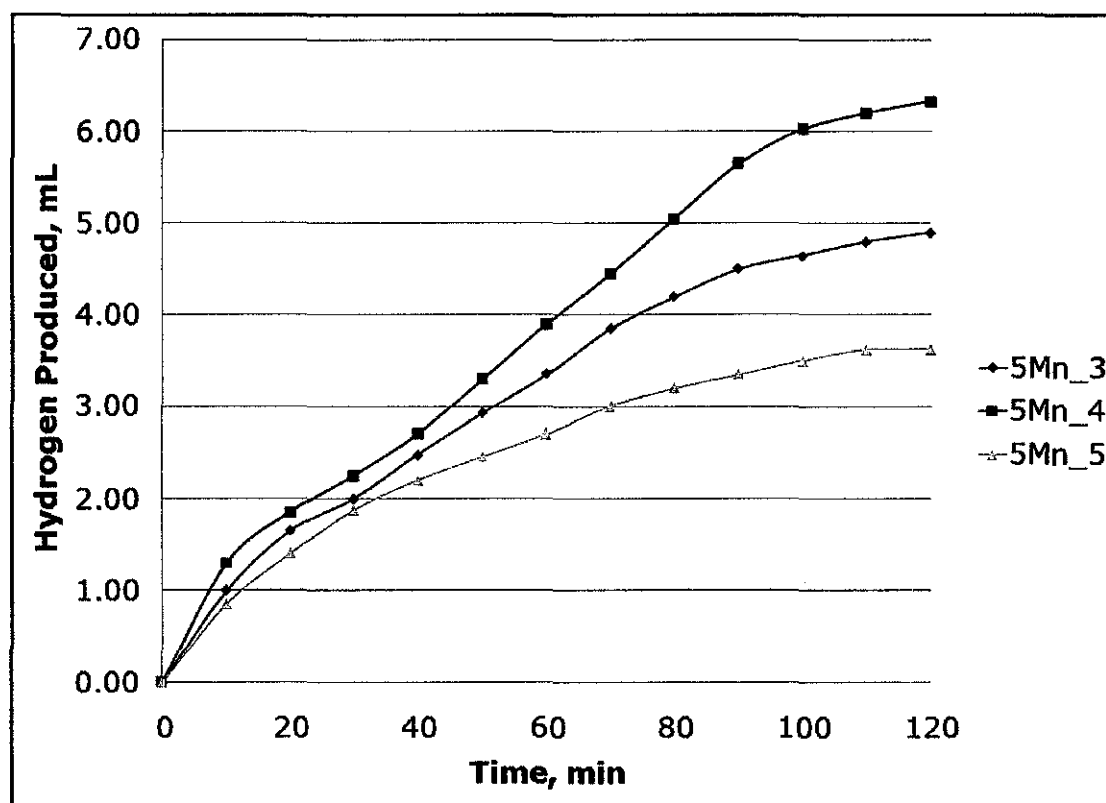

Figure 4.2: The effect of calcination temperature on H_2 production for 2 hours.

The result obtained indicated that the best photocatalyst was 5Mn_4. Further reaction was carried out by using 5Mn_4 photocatalyst in sea water. It is conducted in order to study the effect of electrolyte to the photoactivity. From the experiment done, it was shown that the reaction rate of the photocatalyst is faster by using sea water instead of distilled water especially during initial state of the reaction (better conductivity). The illustration of the reaction rate for 5Mn_4 in distilled water and sea water are shown in Figure 4.3(a). By using sea water, the amount of hydrogen evolved also was higher compared to if using distilled water. This is due to the electrolyte properties in sea water that enhanced the performance of photocatalysts. Figure 4.3(b) shows the overall reaction for 2 hours for both pure titania and 5Mn_4 in distilled water and sea water. The activity of 5Mn_4 showed163% improvement for distilled water and 154% improvement for sea water compared to pure TiO_2.
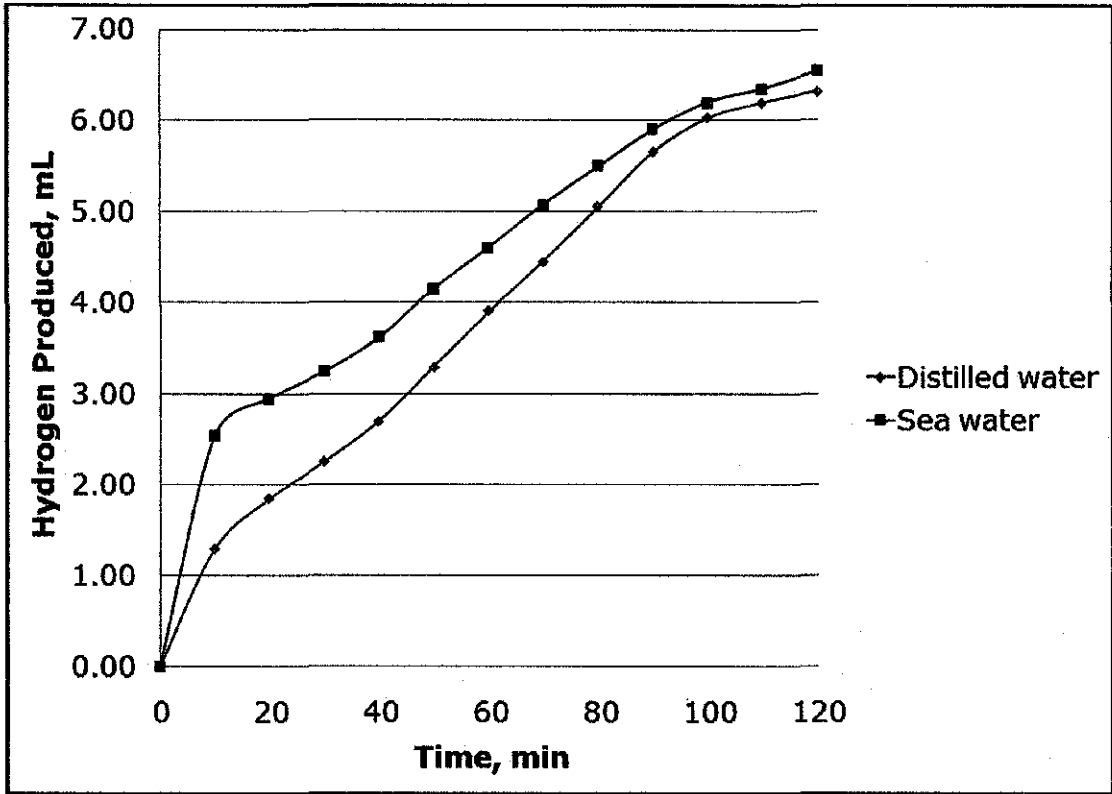
(a)
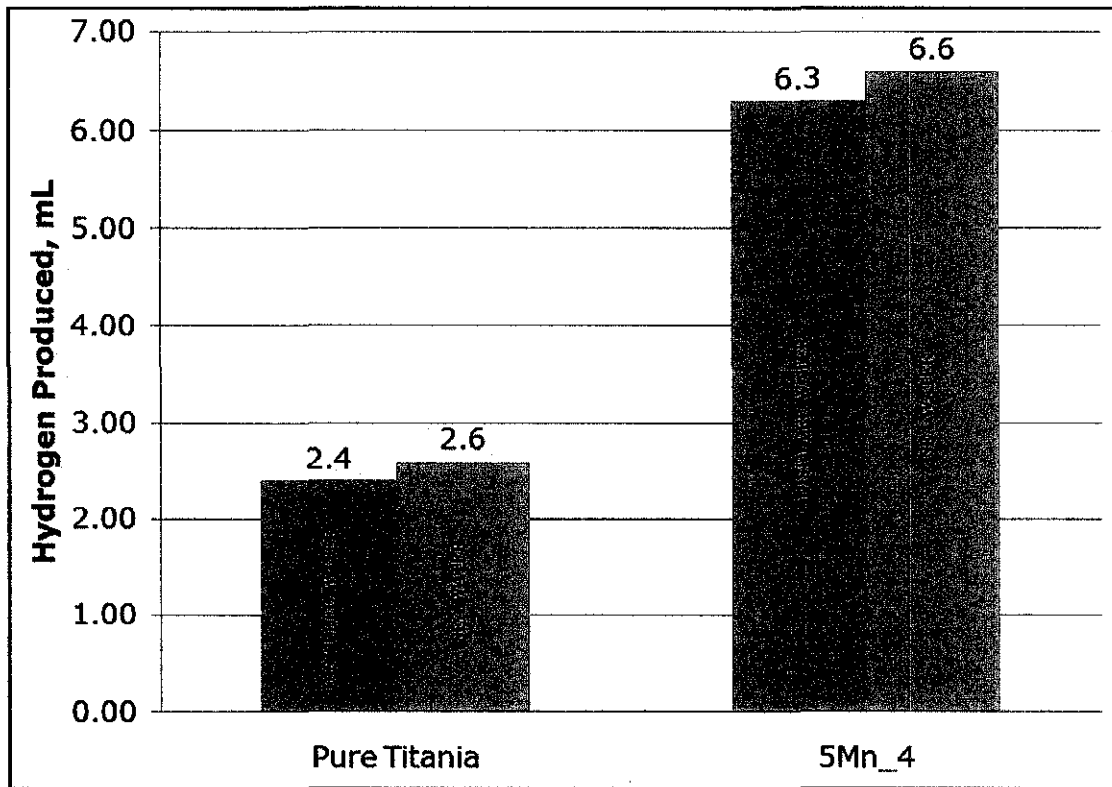
(b)

Figure 4.3: Hydrogen evolved (a) using 5Mn_4 in different reaction medium as a function of time and (b) after 2 hours reaction for pure titania and 5Mn_4 in different reaction medium.

4.2   Catalyst Characteristics

4.2.1   Thermogravimetric analysis (TGA)

Thermogravimetric analysis is performed to determine the thermal behavior of the thermal stability of the photocatalyst. The TGA of raw Mn/TiO_2 photocatalyst samples are presented in weight loss pattern in Figure 4.4. The temperature range is from $30^\circ C$ to $850^\circ C$. The total weight loss estimated for 1 wt% Mn/TiO_2 raw catalyst sample is around 4.2%, for 5 wt% Mn/TiO_2 raw catalyst, the total weight loss is 3.9% and 5.3% Mn/TiO_2 for 10 wt% raw catalyst.

There are two decomposition steps for all samples; one is from $30\ ^\circ C$ to $120\ ^\circ C$ and the other one is from $200\ ^\circ C$ to $500\ ^\circ C$. These are attributed to the evaporation of the physically retained or absorbed water and decomposition of manganese nitrate to form manganese oxide. This TG curves are used to obtain information about the optimum calcinations temperature for the Mn/TiO_2 photocatalyst samples. Based on the TG curves obtained, the calcination temperature chosen is $300\ ^\circ C$, $400\ ^\circ C$ and $500\ ^\circ C$ since the weight loss is not too drastic after $300\ ^\circ C$ which indicates that there is no nitrate group in the samples.
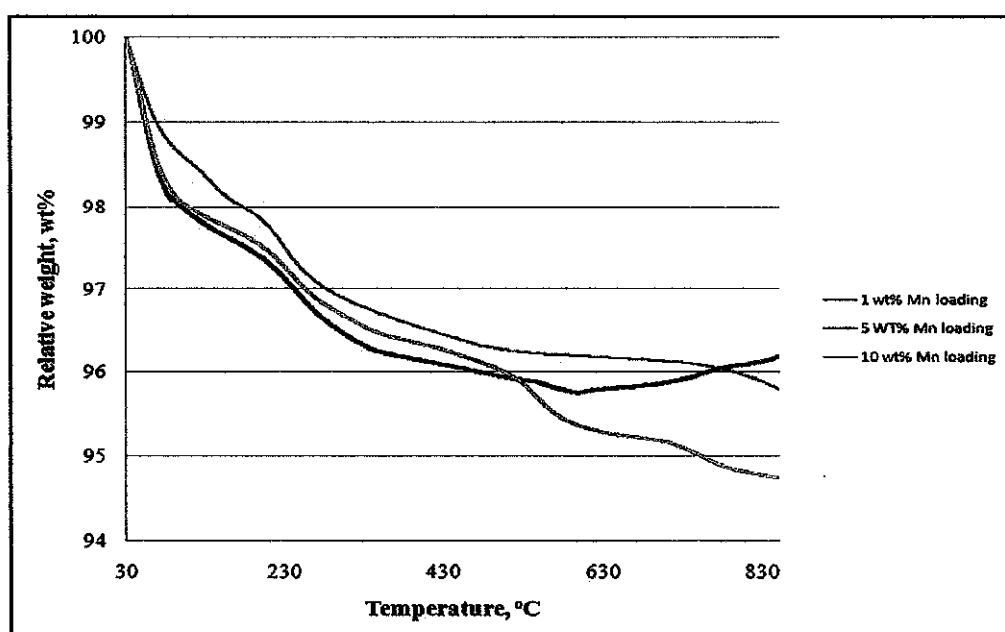
Figure 4.4: The weight loss profile of the Mn metal supported TiO_2 catalyst.

17

4.2.2 Diffuse Reflectance Spectroscopy (DR-UV-Vis)

The DR-UV-Vis spectra of the catalyst samples as well as of pure TiO$_2$ are shown in Figure 4.5. The absorption threshold of pure titania (P25) was ~400nm (UV range). However, this absorption range could be shifted from UV range to visible range (wavelength >400nm) by doping pure titania with manganese metal. It could be observed for all the photocatalyst samples and it is shown in Figure 4.4 below. For an individual DR-UV-Vis result, refer to Appendix B.
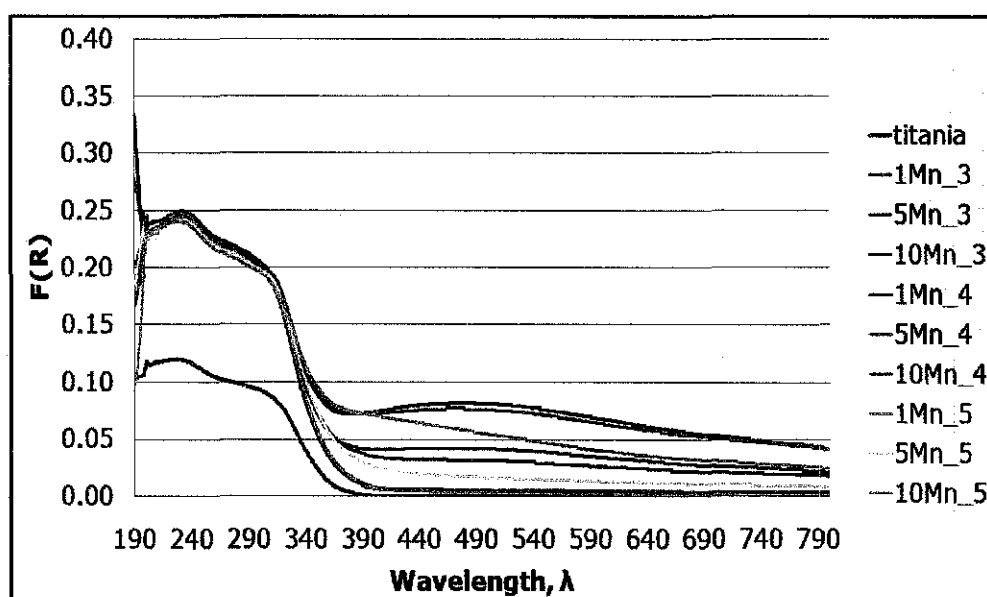

Figure 4.5: DR-UV-Vis spectra of TiO$_2$ and Mn-doped TiO$_2$.

Shifting the absorption band to the visible range can promote the photocatalytic activity of Mn/TiO$_2$. Based on the result obtained, the sensitivity of the photocatalyst towards visible light increases as the temperature decreases with increasing wt% metal doped into pure titania. Thus, it can be concluded here that doping with a transition metal is one of the effective way in order to enhance the hydrogen production under visible light.

From DR-UV-Vis results, band gap energy for each photocatalyst sample was estimated. This could be done by plotting the transformed Kubelka-Munk functions $[F(R).hv]^{1/2}$ versus hv and doing the extrapolation on the plot. The illustration of this Tauc plot is shown in the Figure 4.6. The
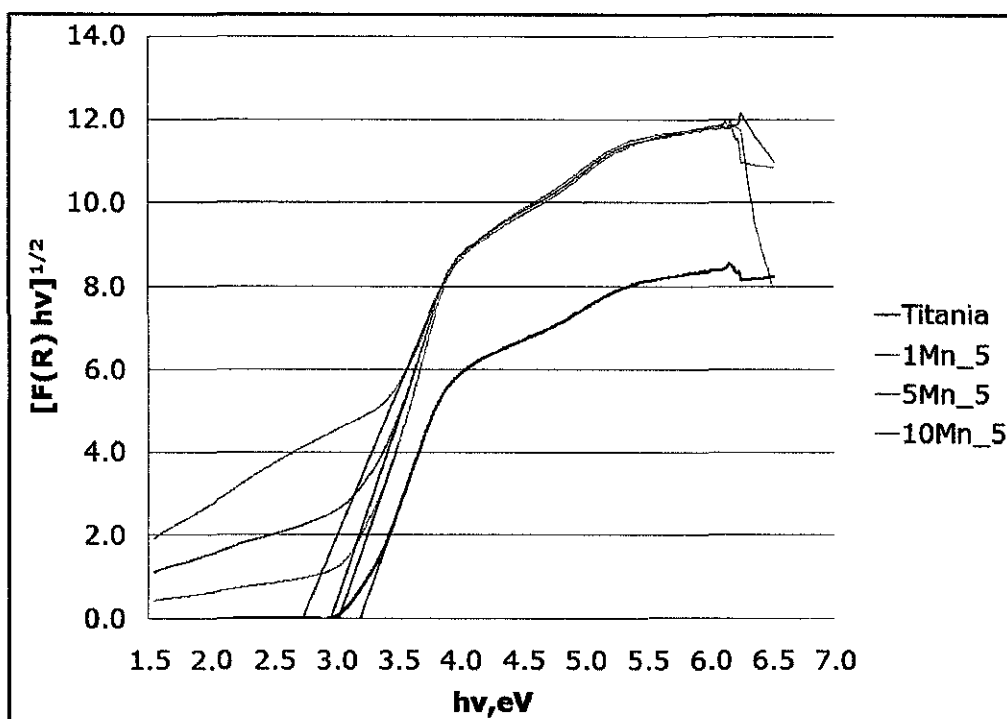
band gap for each sample including pure titania are shown in the Table 4.1. For individual plot of transformed Kubelka-Munk function, refer to Appendix B.
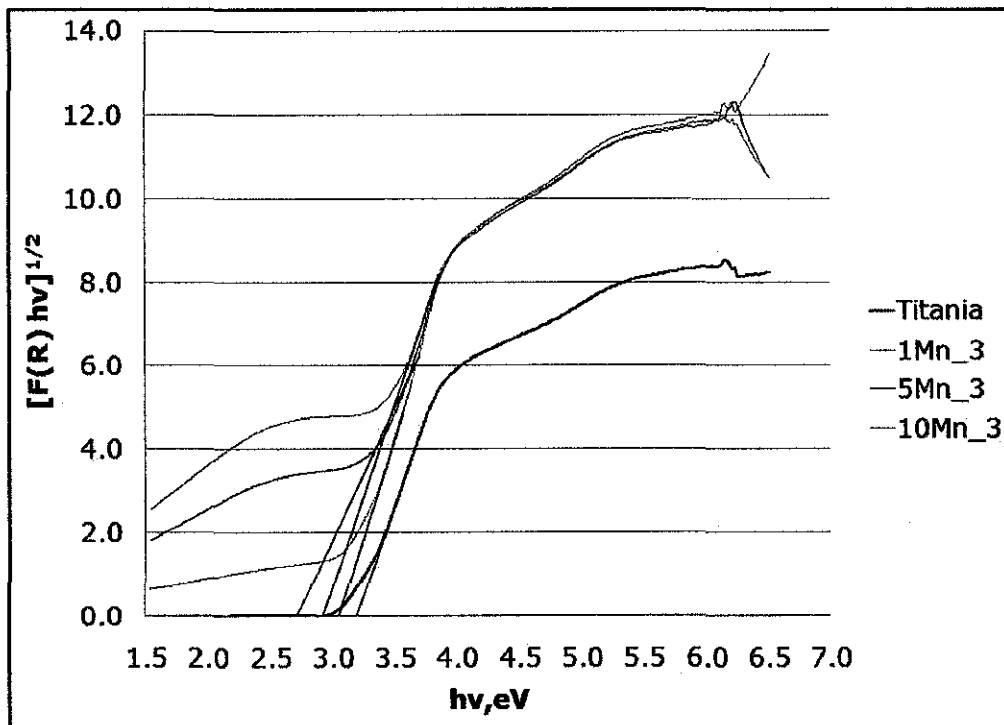
(a)
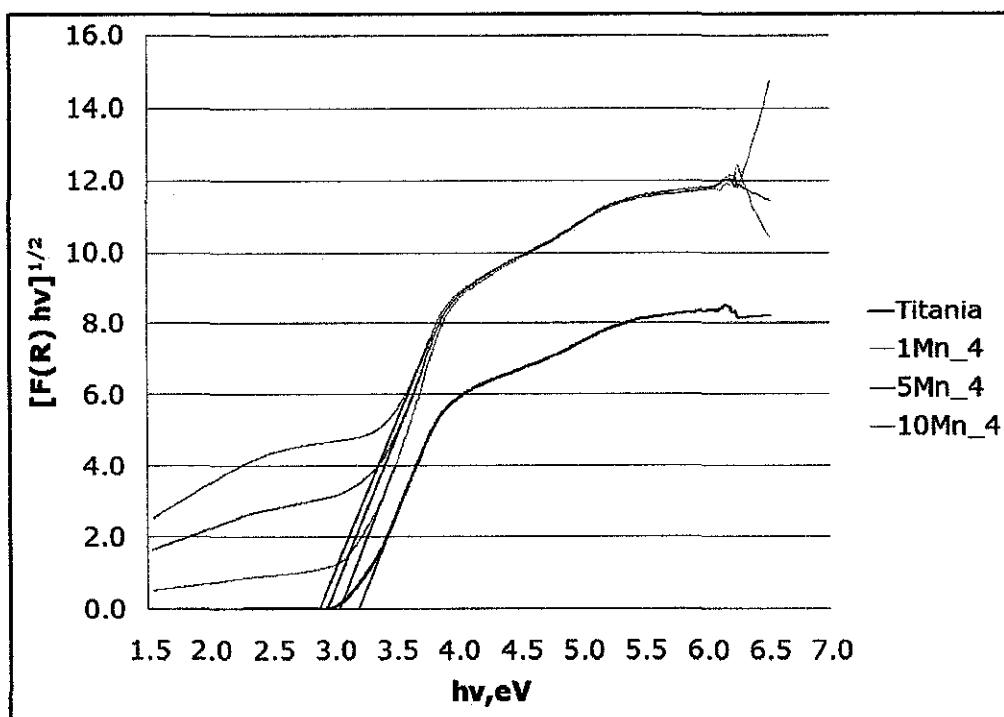
(b)

(c)

Figure 4.6: Plot of transformed Kubelka–Munk functions $[F(R).hv]^{1/2}$ versus hv for Mn/TiO_2 and TiO_2 samples to estimate band gap energies by linear extrapolation after calcinations at (a) 300 °C, (b) 400 °C and (c) 500 °C.

Table 4.1: Band gap energy for each photocatalyst sample.

Photocatalyst	BG Energy
Pure titania	3.20
1Mn_3	3.06
5Mn_3	2.73
10Mn_3	2.93
1Mn_4	3.05
5Mn_4	2.95
10Mn_4	2.89
1Mn_5	3.03
5Mn_5	2.97
10Mn_5	2.74

All the photocatalysts showed that there were reduction in their band gaps compared to TiO_2. The calculated band gap energy for pure TiO_2 is also found to be 3.20eV from the extrapolation of the corresponding plot. By doping titania with manganese metal, the band gap energy reduces. Thus, it

20

could enhance the performance of the photocatalyst in order to produce hydrogen gases under visible light.

4.2.3 Field Emission Scanning Electron Microscopy (FESEM)

Figure 4.7 shows the images of FESEM for 5Mn_3, 5Mn_4 and 5Mn_5. Based on FESEM results, it could be seen how well the Mn metal were doped on titania surface. For 5Mn_3, it showed that the interaction between titania and manganese metal were not well interacted. 300 °C calcination temperature is not enough for Mn metal to be doped onto titania. For 5Mn_5, it could be seen that the titania itself formed cluster between each other and Mn metal could not be doped well onto titania. It means that, the surface area for the reaction to take place were less thus the hydrogen produced also less.

The best interaction between Mn metal and titania could be seen from 5Mn_4. Mn metal was well doped at 400 °C calcinations temperature and the surface area for the reaction to take place also high thus increase the amount of hydrogen gases produced. For more FESEM image, refer to Appendix C.

(a)

21
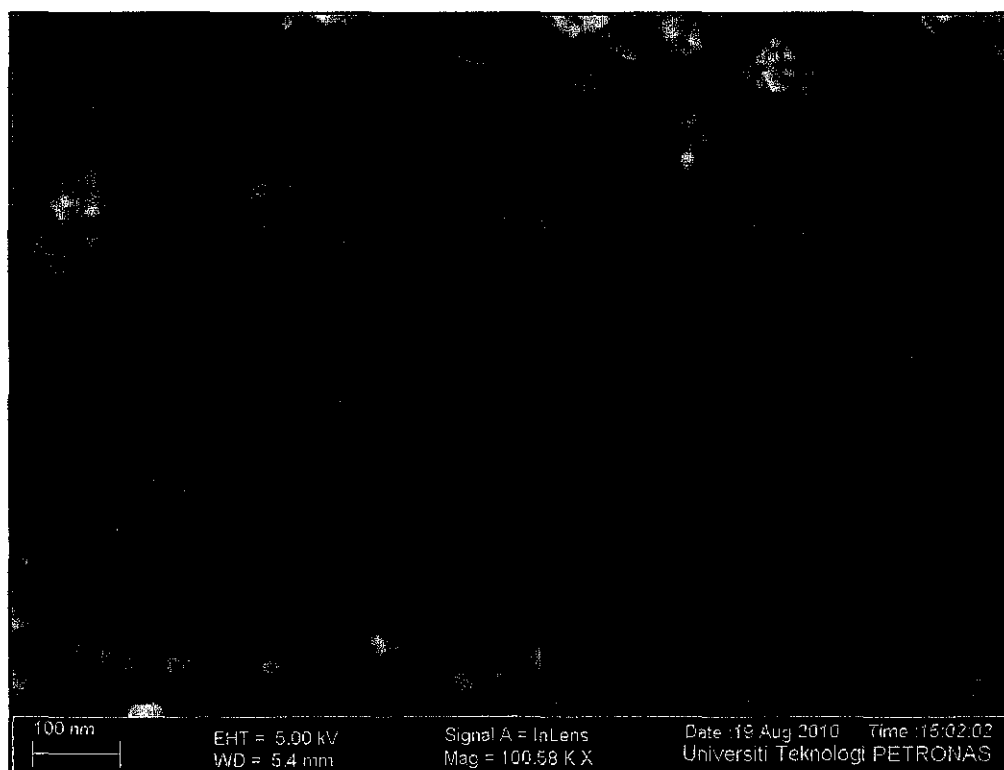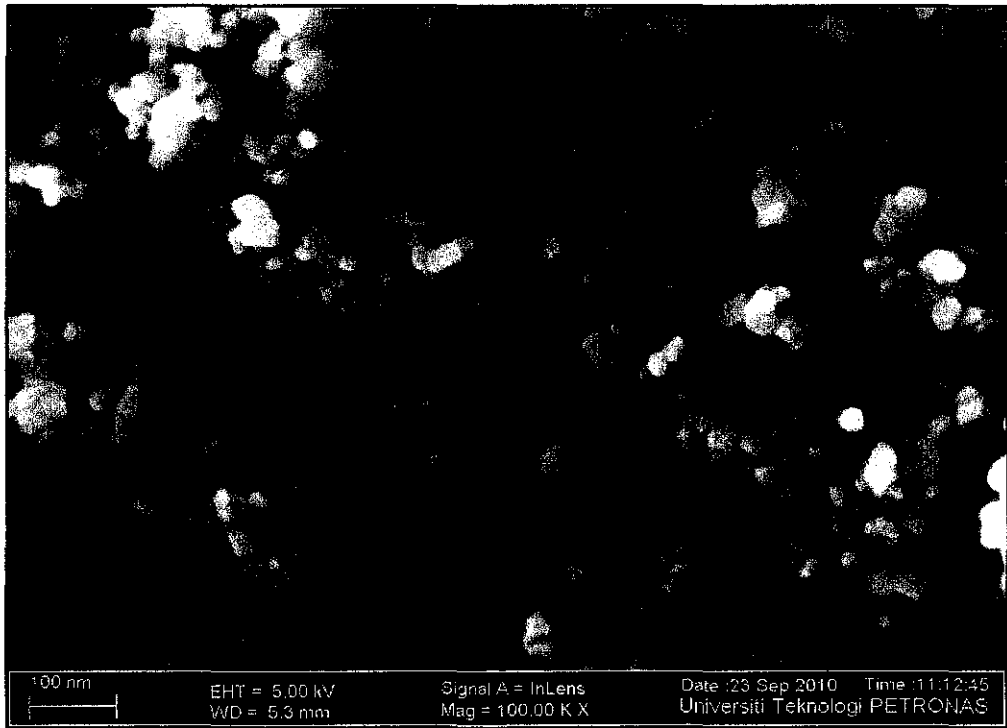
(b)
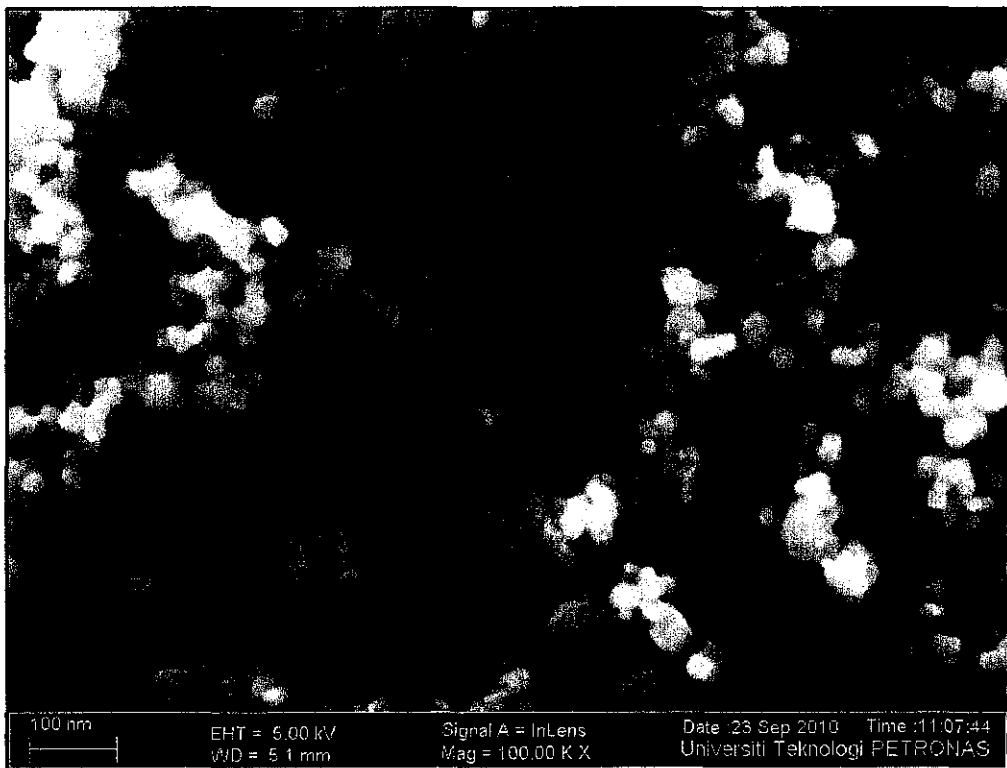
(c)

Figure 4.7: FESEM micrographs of the Mn/TiO2 photocatalysts for (a)5Mn_3, (b)5Mn_4 and (c)5Mn_5.

4.2.4 Fourier Transform Infra-Red (FTIR) Spectra

The FTIR transmission spectra of the Mn/TiO_2 photocatalyst before calcination and after calcination temperature (300 °C, 400 °C and 500 °C) are shown in Figure 4.8. As shown in Figure 4.8 (a), there are absorption peaks around 1600 cm^{-1} and 3400 cm^{-1}. Peaks around 1600 cm^{-1} are attributed to O-H bending while peaks around 3400 cm^{-1} are corresponding to O-H stretching. The IR band from 400 cm^{-1} to 900 cm^{-1} are representing Ti-O stretching vibrations (Yan *et al.*, 2004; Yoong *et al.*, 2009).

The presence of nitrate (NO_3^-) group can be observed from the absorption peak at 1384 cm^{-1}. All of uncalcined samples show the presence of nitrate group in the samples. There is also peak at around 2300 cm^{-1} for some samples. This peak is attributed to carbon dioxide, CO_2 that exists in atmosphere. However, not all samples have the peak at that 2300 cm^{-1} due to the CO_2 concentration that does not fix at certain time where it always changing.

Same goes to Figure 4.7 (b), Figure 4.7 (c) and Figure 4.7 (d) where all of the samples show the same patterns which there are absorption peaks around 1600 cm^{-1}, 2300 cm^{-1}, 3400 cm^{-1} and from 400 cm^{-1} to 900 cm^{-1}. Peaks around 1600 cm^{-1} and 3400 cm^{-1} are attributed to O-H bending and stretching respectively. Peak at around 2300 cm^{-1} is attributed to CO_2 in atmosphere and absorption band from 400 cm^{-1} to 900 cm^{-1} are representing Ti-O stretching vibrations.
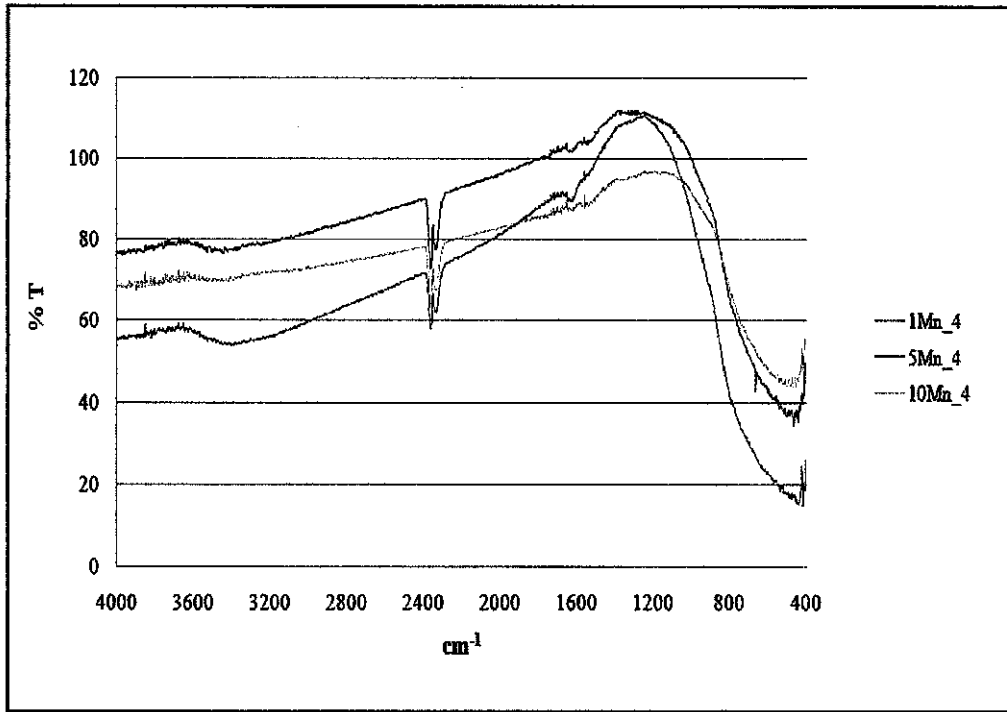
However, for calcined samples, there is no absorption band at 1384cm^{-1} which is corresponding to the presence of NO_3^- group. This is indicating that nitrate group is completely removed from raw catalyst by calcinations process at 300 °C, 400 °C and 500 °C calcinations temperature.
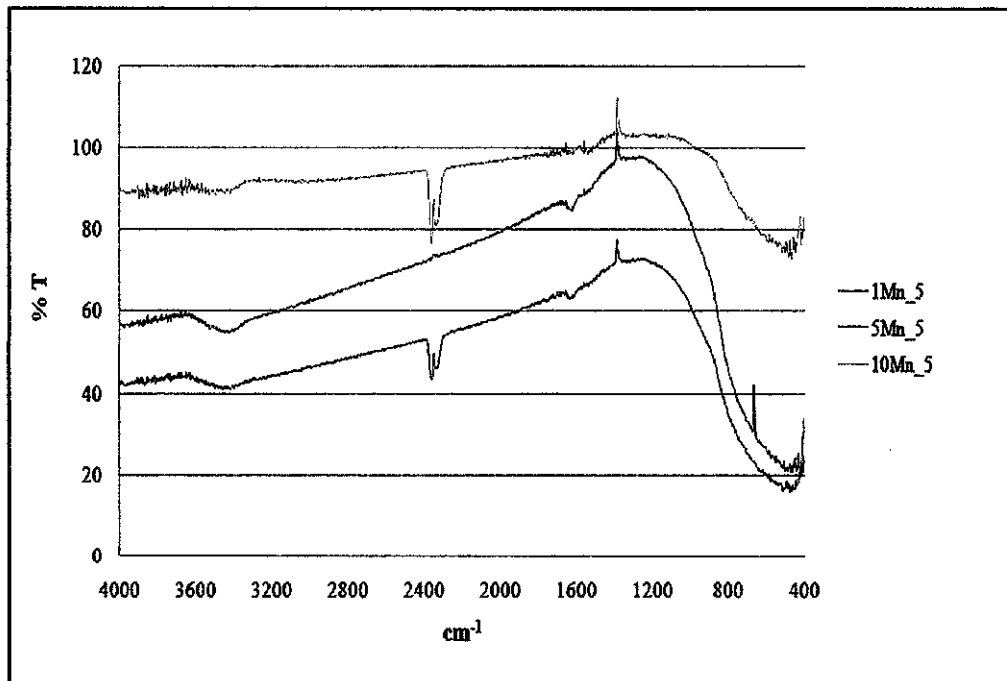
23

(a)

(b)

24
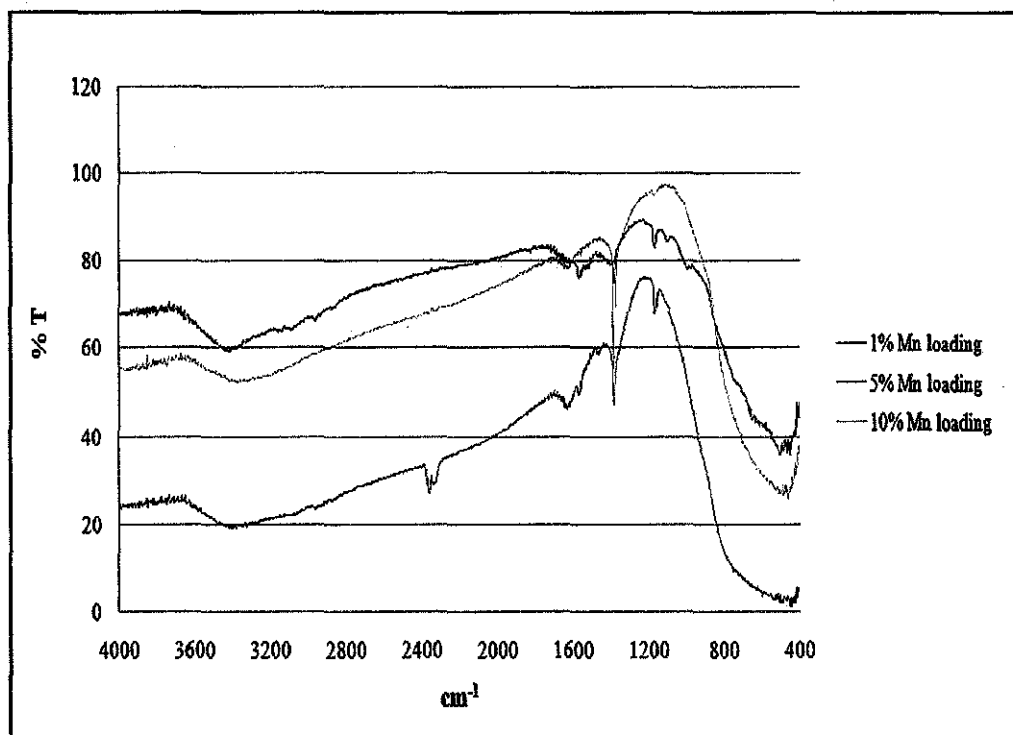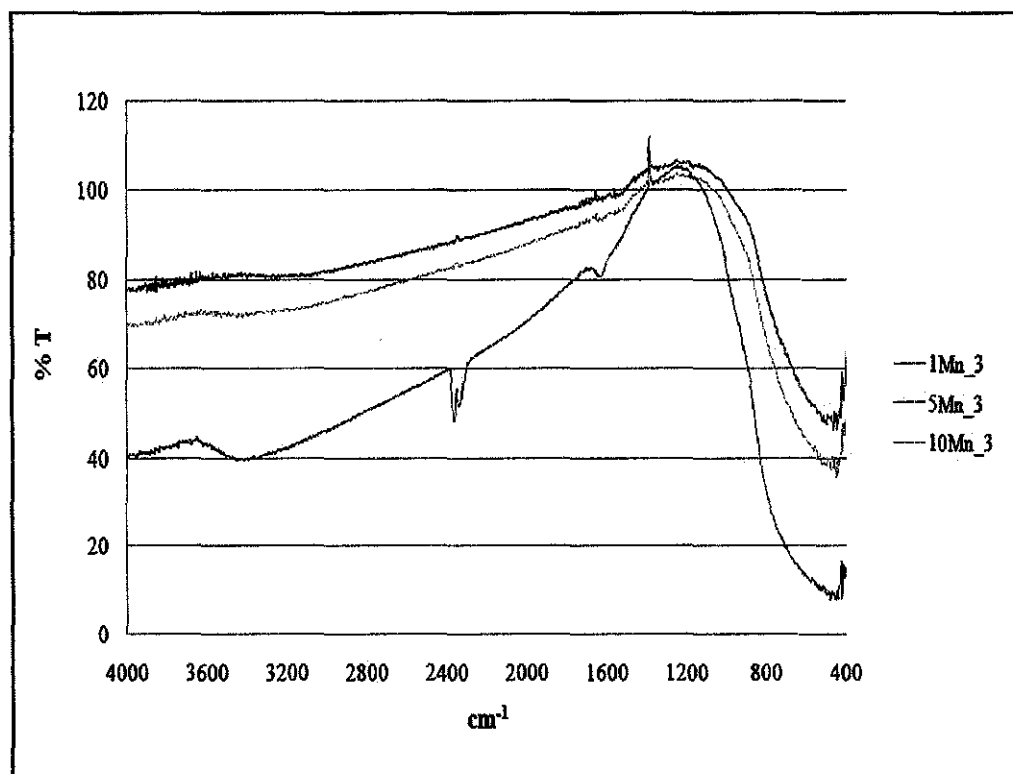
(c)

(d)

Figure 4.8: FTIR transmission spectra for Mn/TiO$_2$ photocatalyst (a) before calcination and after calcination at (b) 300 °C (c) 400 °C and (d) 500 °C.

4.2.5 X-ray Diffusion (XRD)

The XRD patterns of the Degussa P25 and Mn/ TiO_2 photocalysts are shown in Figure 4.9. There are peaks at $2\theta=25.2°$ and $2\theta=27.5°$ appear in all samples. These two peaks correspond to the main peak of anatase and rutile, respectively. It is notable that only anatase and rutile phase was observed without brookite phases in all of the modified samples. Peak shifting is not observed even in 10Mn_5 sample, this indicates that high metal loading and high calcination temperature does not give significant changing to the titania lattice. There is also no Mn peak observed because it is below XRD indication limit and it is showing that Mn metal was highly dispersed on TiO_2. For all samples, the blue line refers to the rutile phase, the red line refers to anatase phase and the black line is referring to the sample.
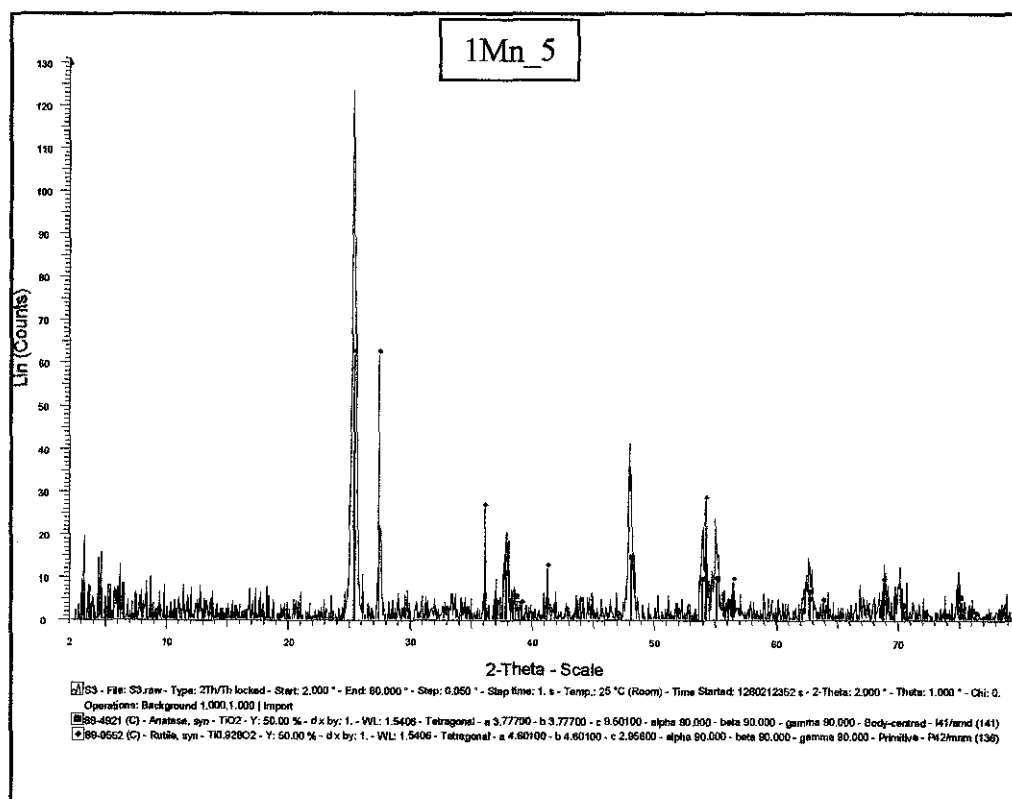
(a)
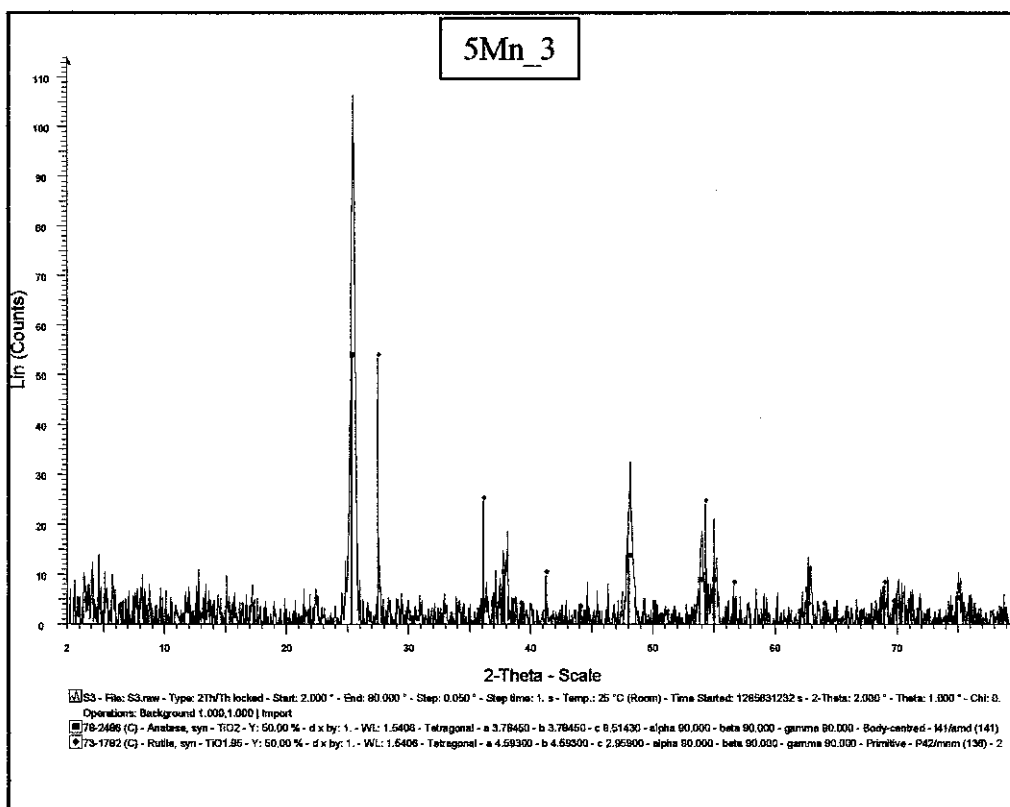
(b)
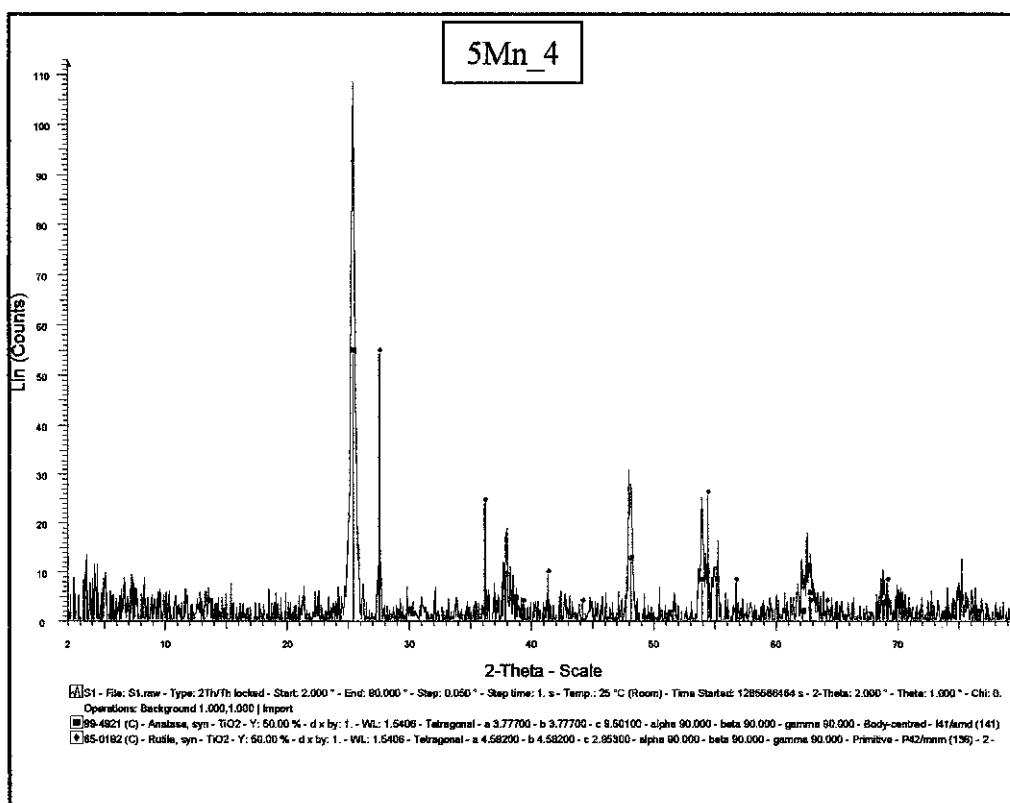
(c)
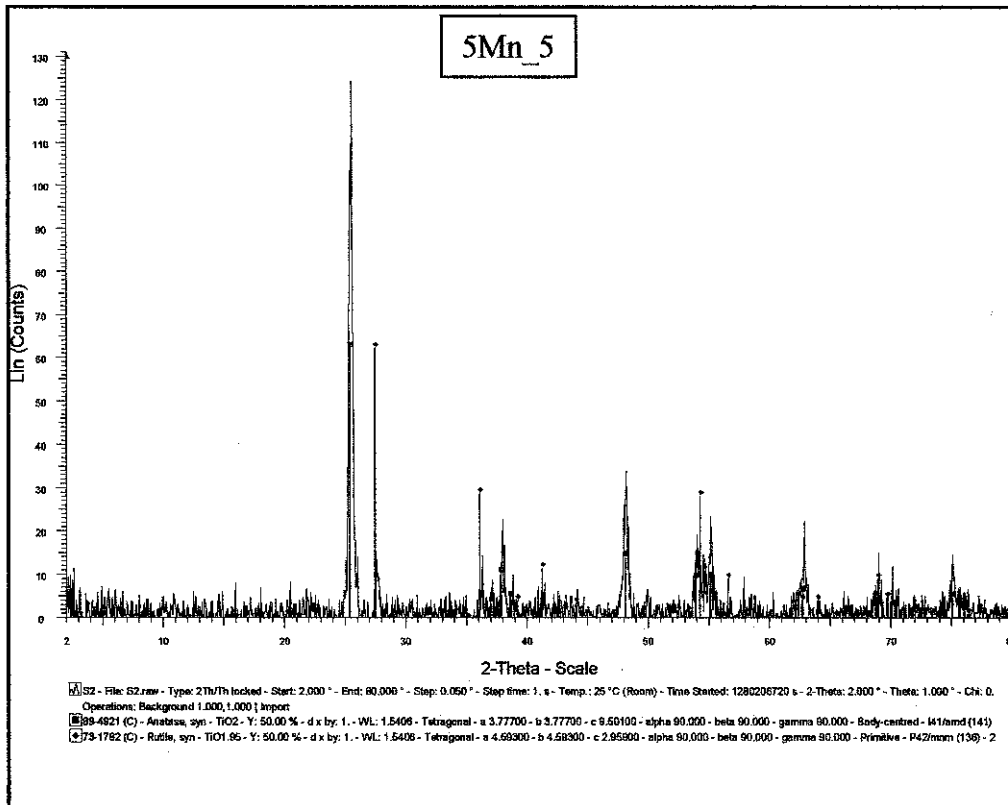
(d)

(e)
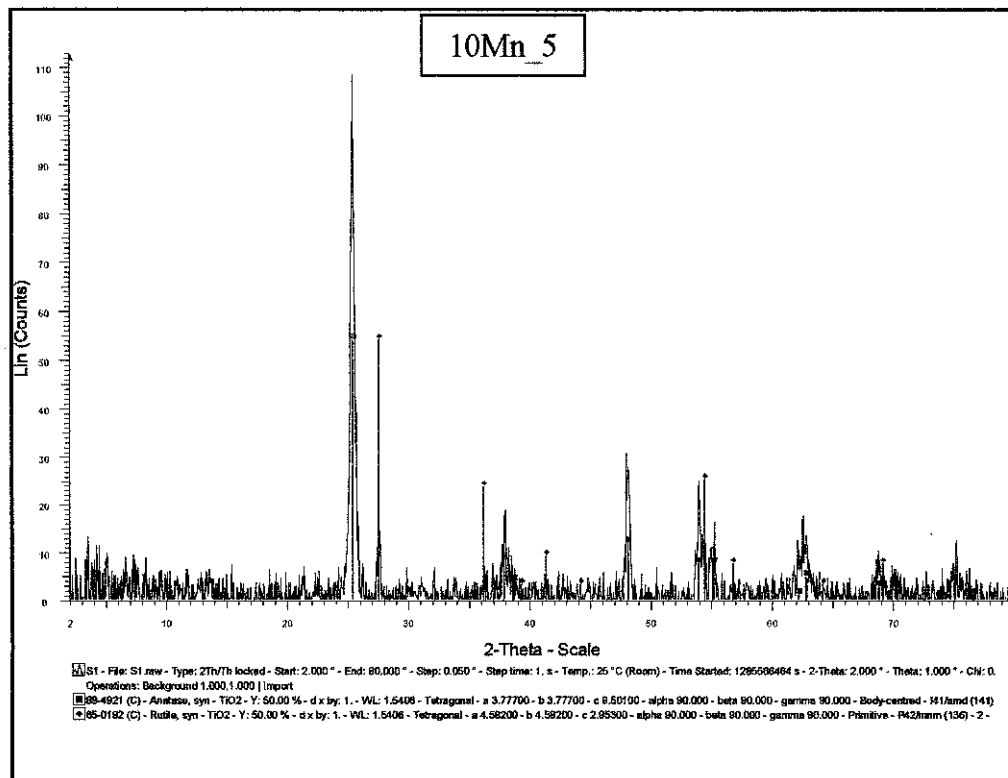
Figure 4.8: XRD difractograms for (a) 1Mn_5 (b) 5Mn_3 (c) 5Mn_4 (d) 5Mn_5 and (e) 10Mn_5.

CHAPTER 5 : CONCLUSION AND RECOMMENDATION

5.1   Conclusion

Overall, it can be concluded that 5Mn_4 produced the highest amount of H_2. The modification that is done to titania photocatalyst has increase its efficiency by making it be able to be active under visible light. Doping titania with Mn has shifted the absorption edge of titania from UV region to visible region to optimize its properties for hydrogen production. By producing hydrogen with this method, hydrogen can be produced without worrying the environmental issue since it is environmental friendly. It can contribute good things to the industries and users.

5.2   Recommendation

Further studies are recommended based on the result obtained from this research. In order to increase the performance of the photocatalyst, the future study can be done by varying:

- ❖ the types and number of metal ion doped to TiO_2
- ❖ the photocatalyst preparation method
- ❖ the calcination temperature and calcination time

All those factors might be giving effect to the photocatalyst activity. However, more literature review needs to be studied continuously in order to understand more about this experimental works and get the best result for the project.

REFERENCES

Bae S.W., Borse P. H., Hong S. J., Jang S. J. & Lee J. S. (2007). Photophysical properties of nanosized metal-doped TiO₂ photocatalyst working under visible light. *Journal of the Korean Physical Society, 51*, S22-S26

Baojiang, L., Xubang, C., & Jinxin, H. (2009). *II.K.10 Fundamental Investigations of Water Splitting on Model TiO$_2$ Photocatalysts Doped for Visible Light Absorption,* http://www.hydrogen.energy.gov/pdfs/progress08/ii_k_10_henderson. pdf, 28 February 2010.

Brezová, V., Blazková, A., Karpinský, L., Grosková, J., Havlínová, B., Jorík, V., et al. (1997). Phenol decomposition using Mn^{+}/TiO₂ photocatalysts supported by the sol-gel technique on glass fibres. *Journal of Photochemistry and Photobiology A: Chemistry, 109*(2), 177-183.

Choi, W.Y., Termin, A. & Hoffmann, M. R. (1994). The role of metal ion dopants in quantum-sized TiO₂: correlation between photoreactivity and charge carrier recombination dynamics, *J Phys Chem, 98* (51), 13669–13679.

Collodi, G., Wheeler, F. (2009). Hydrogen production via steam reforming with CO₂ capture. (http://www.aidic.it/CISAP4/webpapers/7Collodi.pdf)

Dholam, R., Patel, N., Adami, M., & Miotello, A. (2009). Hydrogen production by photocatalytic water-splitting using Cr- or Fe-doped TiO₂ composite thin films photocatalyst. *International Journal of Hydrogen Energy, 34*(13), 5337-5346.

Dvoranová, D., Brezová, V., Mazúr, M., & Malati, M. A. (2002). Investigations of metal-doped titanium dioxide photocatalysts. *Applied Catalysis B: Environmental, 37*(2), 91-105.

Elvington, M., Brown, J., Arachchige, S.M., & Brewer, K., J. (2007). Photocatalytic Hydrogen Production from Water Employing A Ru, Rh, Ru Molecular Device for Photoinitiated Electron Collection. *Journal of the American Chemical Society, 129* (35), 10644-10645.

Hu, J., Chu, W., & Shi, L. (2008). Effects of carrier and mn loading on supported manganese oxide catalysts for catalytic combustion of methane. *Journal of Natural Gas Chemistry, 17*(2), 159-164.

National Energy Education Development Project, (2009). *Secondary energy book: Hydrogen*, http://www.need.org/EnergyInfobooks.php, 20 March 2010.

Jeong, H., Kim, T., Kim, D., & Kim, K. (2006). Hydrogen production by the photocatalytic overall water splitting on $NiO/Sr_3Ti_2O_7$: Effect of preparation method. *International Journal of Hydrogen Energy, 31*(9), 1142-1146.

Jin, M., Nagaoka, Y.,Nishi, K., Ogawa, K., Nagahata, S., Horikawa, T., Katoh, M., Tomida, T., & Hayashi, J. (2008). Adsorption Properties and photocatalytic activity of TiO_2 and La-doped TiO_2. *Adsorption, 14*, 257-263.

Katoh, M., Aihara, H., Horikawa, T., & Tomida, T. (2006). Spectroscopic study for photocatalytic decomposition of organic compounds on titanium dioxide containing sulfur under visible light irradiation. *Journal of Colloid and Interface Science, 298*(2), 805-809.

Kitano, M., Tsujimaru, K., & Anpo, M. (2006). Decomposition of water in the separate evolution of hydrogen and oxygen using visible light-responsive TiO_2 thin film photocatalysts: Effect of the work function of the substrates on the yield of the reaction. *Applied Catalysis A: General, 314*(2), 179-183.

Li, Y., Peng, S., Jiang, F., Lu, G. & Li, S. (2007). Effect of doping TiO_2 with alkaline-earth metal ions on its photocatalytic activity. *Directory of Open Access Journal, 72* (4), 393-402

Lin, C. H., Lee, C. H., Chao, J. H., Kuo, C.Y., Cheng, Y. C., Huang, W. N., Chang, H.W., Huang, Y. M. & Shih, M. K. (2004). Photocatalytic generation of H_2 gas from neat ethanol over Pt/TiO_2 nanotube catalysts. *Catalysis Letters*, 98 (1), 61-66

Liu, A. R., Wang, S. M., Zhao, Y. R., & Zheng, Z. (2006). Low-temperature preparation of nanocrystalline TiO_2 photocatalyst with a very large specific surface area. *Materials Chemistry and Physics, 99*(1), 131-134.

Liu, M., You, W., Lei, Z., Takata, T., Domen, K., & Li, C. (2006). Photocatalytic water splitting to hydrogen over a visible light-driven $LaTaON_2$ catalyst. *Chinese Journal of Catalysis, 27*(7), 556-558.

Liu, Y., Luo, M., Wei, Z., Xin, Q., Ying, P., & Li, C. (2001). Catalytic oxidation of chlorobenzene on supported manganese oxide catalysts. *Applied Catalysis B: Environmental, 29*(1), 61-67.

Papp, J., Shen, H. S., Kershaw, R., Dwight, K. & Wold, A. (1993). Titanium (IV) oxide photocatalyst with palladium. *Chemistry Material, 5,* 284-288.

Seyler, M., Stoewe, K., & Maier, W. F. (2007). New hydrogen-producing photocatalysts—A combinatorial search. *Applied Catalysis B: Environmental, 76*(1-2), 146-157.

Sreekanth, P. M. & Smirniotis, P. G. (2008). Selective reduction of NO with CO over titania supported transition metal oxide catalyst. *Catalyst Letters,* 122 (1), 37-42.

Sreethawong, T., Junbua, C., & Chavadej, S. (2009). Photocatalytic H_2 production from water splitting under visible light irradiation using eosin Y-sensitized mesoporous-assembled Pt/TiO_2 nanocrystal photocatalyst. *Journal of Power Sources, 190*(2), 513-524.

Teratani, S., Nakamichi, J., Taya, K., & Tanaka, K. (1982). Bull. Chem. Soc. Jpn. 55, 1688.

Wang, X., Maeda, K., Thomas, A., Takanabe, K., Xin, G., Carlsson, J., M., Domen, K., & Antonietti, M. (2009). A metal-free polymeric photocatalyst for hydrogen production from water under visible light. *Nature Materials, 8,* 76-80.

Wu, Z., Jiang, B., Liu, Y., Wang, H. & Jin, R. (2007). DRIFT study of manganese titania based catalyst for low temperature selective catalytic reduction of NO with NH_3. *Environmental Science & Technology,* 41 (1), 5812-5817.

Xin, W. S., Zhi, M., Ning, W. Y., Zhou, Q. X., & Cheng, L. Z. (2004). Photocatalyic Redox Activity of Doped Nanocrystalline TiO_2. *Acta Phys. –Chim. Sin.* 20 (2), 138-143

Yan, X., He, J., Evans, D. G., Zhu, Y., & Duan, X. (2004). Preparation, characterization and photocatalytic activity of TiO2 formed from mesoporous precursor. *J Porous Mat, 11*(1), 131-139.

Yoong, L. S., Chong, F. K., & Dutta, B. K. (2009). Development of copper-doped TiO_2 photocatalyst for hydrogen production under visible light. *Energy, 34*(10), 1652-1661.

Zhang, L., Kanki, T., Sano, N., & Toyoda, A. (2003). Development of TiO_2 photocatalyst reaction for water purification. *Separation and Purification Technology, 31*(1), 105-110.

Zhang, S., Zhao, Z., Liu, C., Dong, W., Zhang, X., Chen, W. (2004). Study on the optical properties of Mn-doped TiO_2 thin films. *Journal of Material Science,* 39, 2909 – 2910.

APPENDIX A

Calculation for 1 wt% Mn loading

The amount of sample prepared $= 25$ g

Molecular weight $Mn(NO_3).6H_2O$ $= 178.98$ g/mol

Amount of manganese metal needed $= 0.01(25$ g$)$

     $= 0.25$ g Mn

Thus, amount of TiO_2 (Degussa P25) $= 25$ g $- 0.25$ g

     $= 24.75$ g

No. of mol for Mn in 1 mol $Mn(NO_3).xH_2O$

$= 1$ mol

178.98 g $Mn(NO_3).6H_2O$ gives 54.94 g Mn(II)

Thus, the **amount of $Mn(NO_3).6H_2O$** needed for 0.25 g Mn

$= (178.98$ g $/ 54.94$ g$)$ x 0.25 g

$= 0.8144$ g

Calculation for 5 wt% Mn loading

The amount of sample prepared   = 25 g

Molecular weight $Mn(NO_3).6H_2O$ = 178.98 g/mol

Amount of manganese metal needed   = 0.05(25 g)

    = 1.25 g Mn

Thus, amount of TiO_2 (Degussa P25)   = 25 g – 1.25 g

    = 23.75 g

No. of mol for Mn(II) in 1 mol $Mn(NO_3).6H_2O$

= 1 mol

178.98 g $Mn(NO_3).6H_2O$ gives 54.94 g Mn

Thus, the **amount of $Mn(NO_3).6H_2O$** needed for 1.25 g Mn

= (178.98 g / 54.94 g) x 1.25 g

= 4.072 g

Calculation for 10 wt% Mn loading

The amount of sample prepared   = 25 g

Molecular weight $Mn(NO_3).6H_2O$ = 178.98 g/mol

Amount of manganese metal needed   = 0.10(25 g)

                                          = 2.50 g Mn

Thus, amount of TiO_2 (Degussa P25)   = 25 g – 2.50 g

                                          = 22.50 g

No. of mol for Mn in 1 mol $Mn(NO_3).xH_2O$

= 1 mol

178.98 g $Mn(NO_3).xH_2O$ gives 54.94 g Mn

Thus, the **amount of $Mn(NO_3).6H_2O$** needed for 2.50 g Mn

= (178.98 g / 54.94 g) x 2.50 g

= 8.1443 g

APPENDIX B
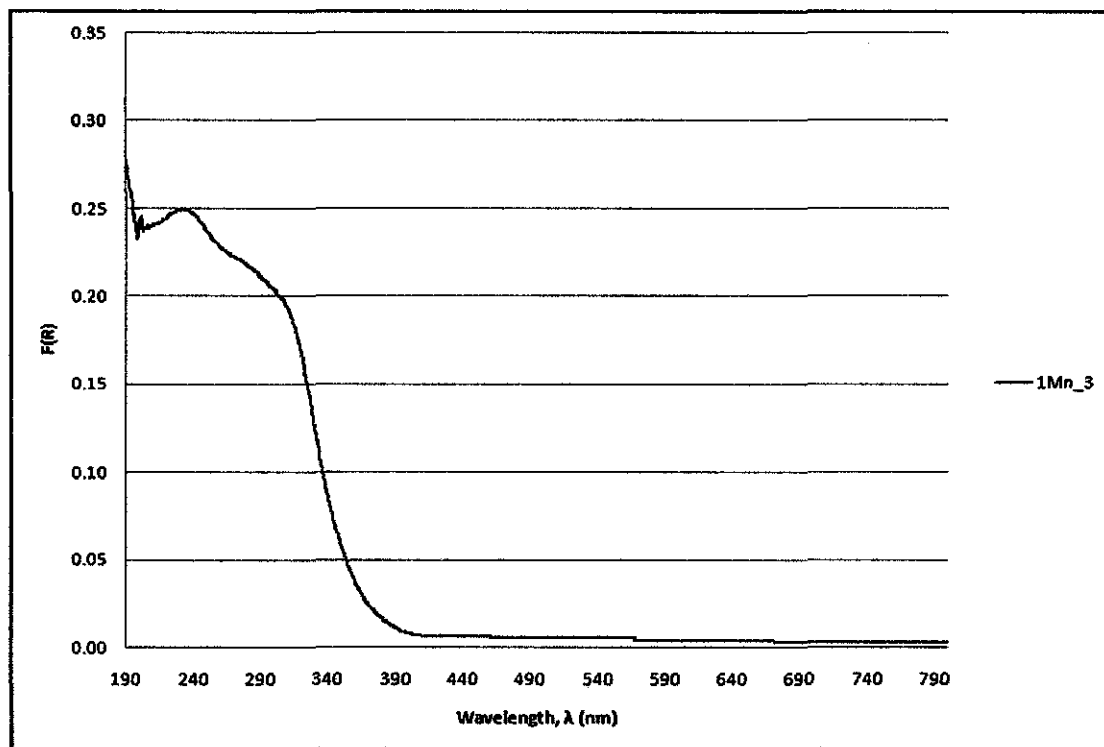
Figure B.1: DR-UV-Vis spectra of 1Mn_3.
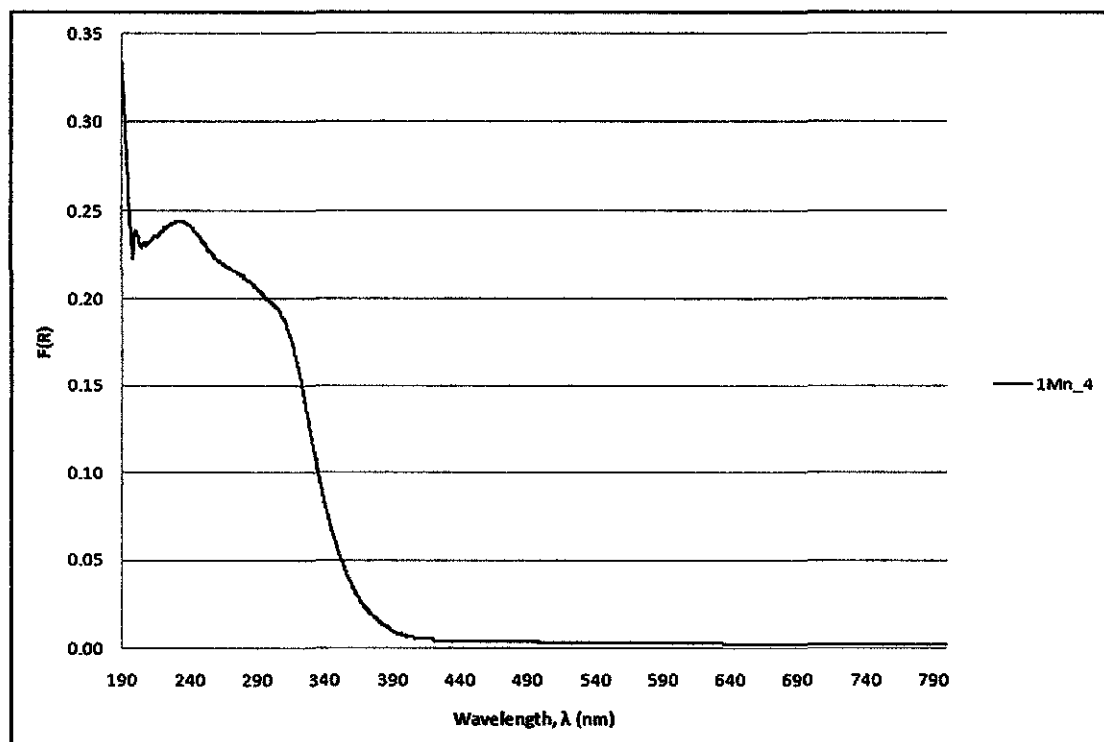
Figure B.2: DR-UV-Vis spectra of 1Mn_4.

37
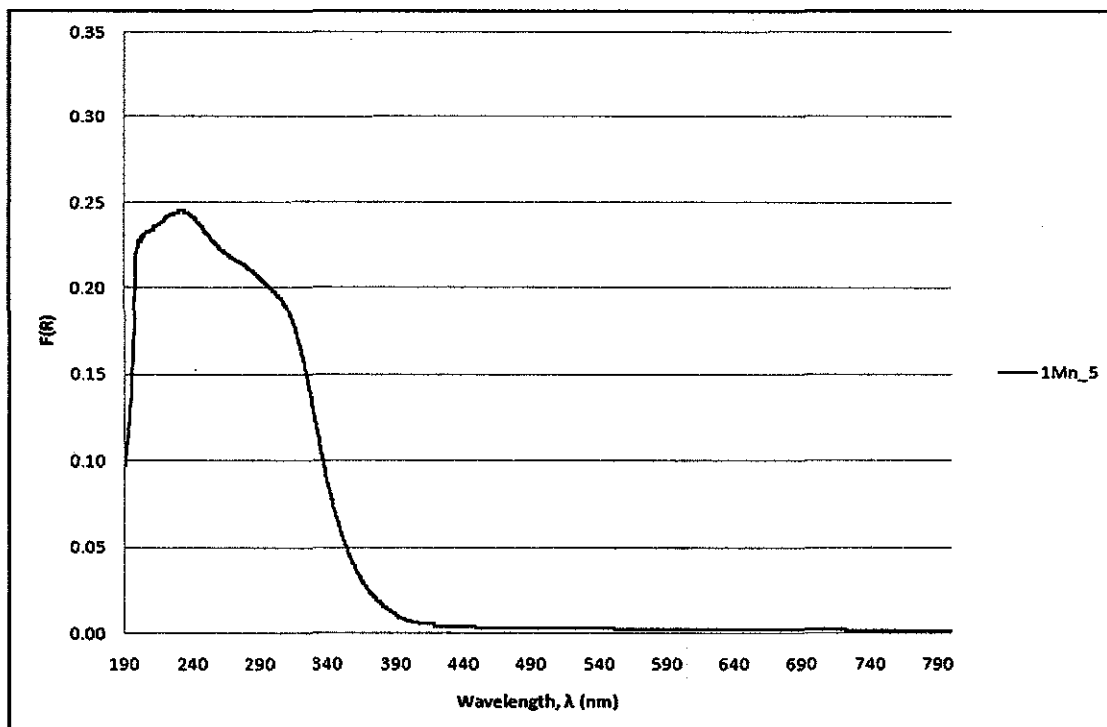
Figure B.3: DR-UV-Vis spectra of 1Mn_5.
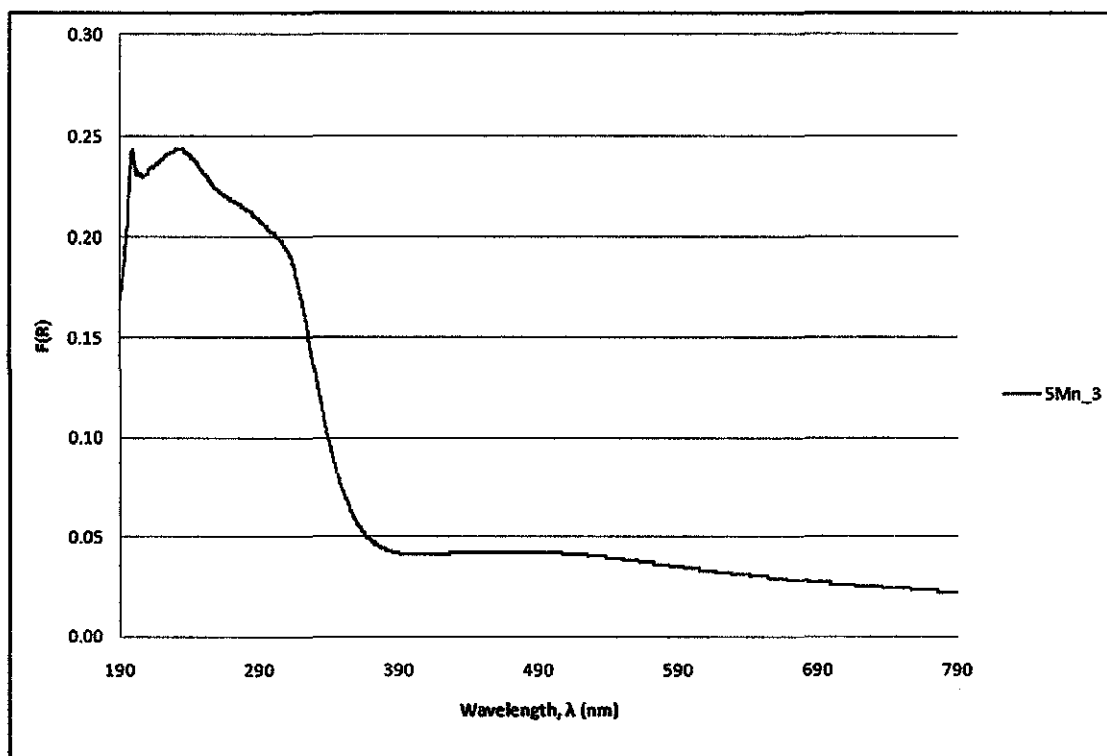
Figure B.4: DR-UV-Vis spectra of 5Mn_3.

38
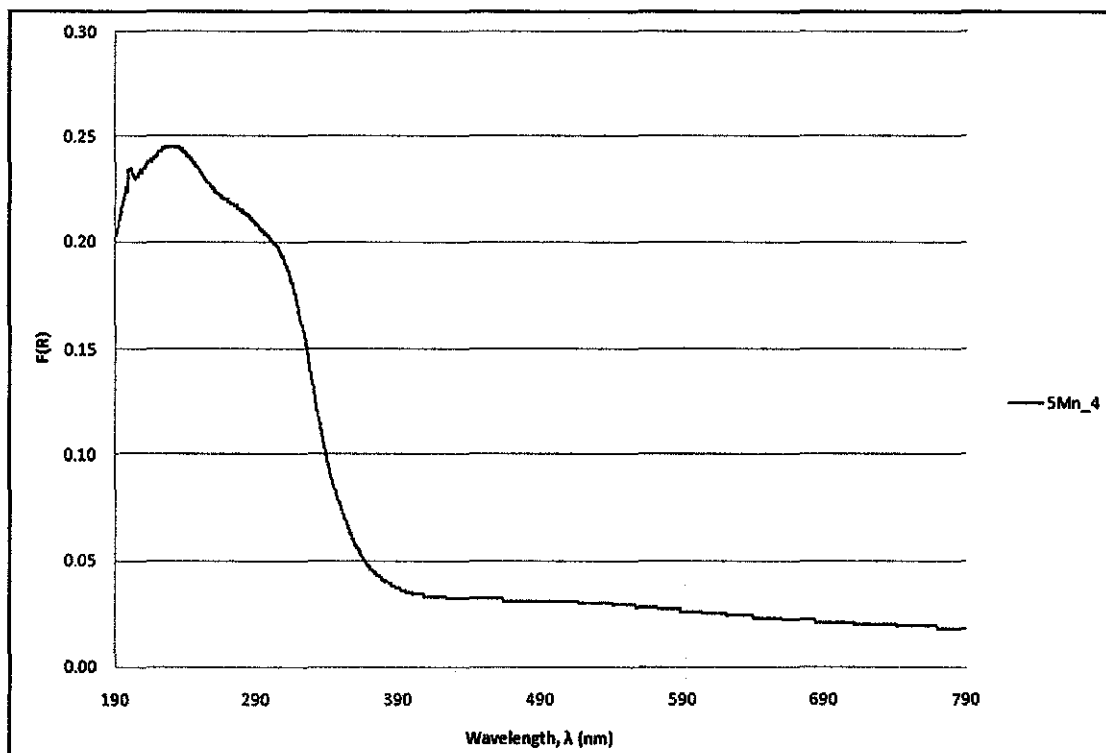
Figure B.5: DR-UV-Vis spectra of 5Mn_4.
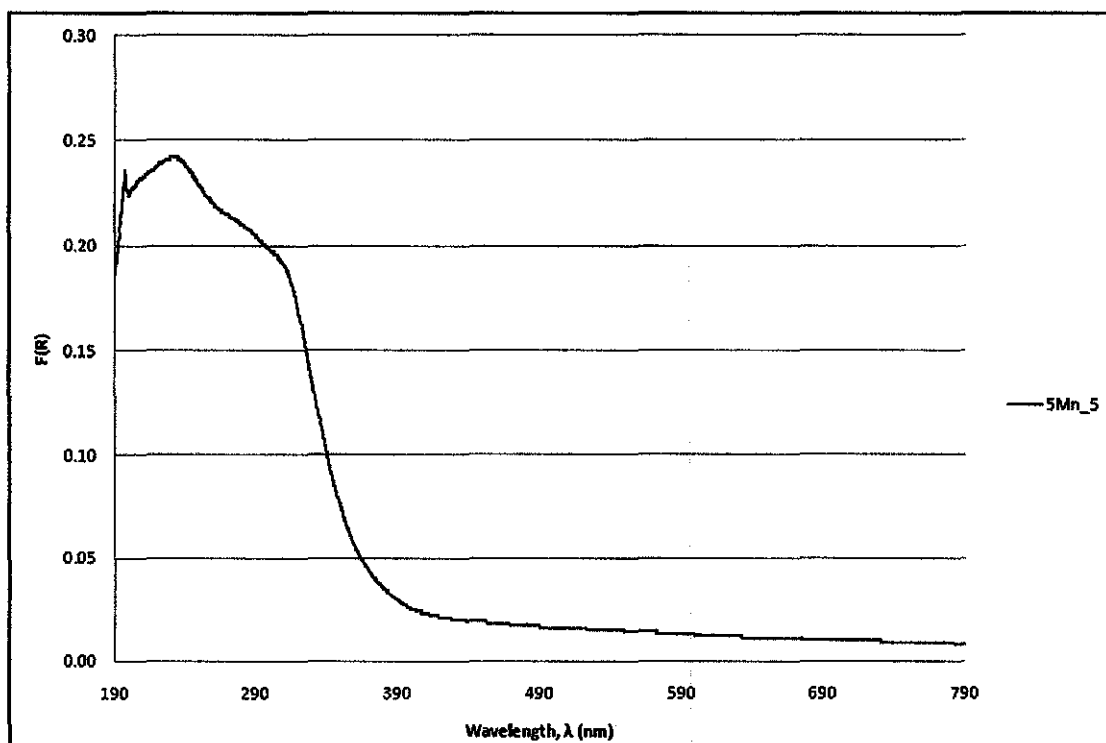
Figure B.6: DR-UV-Vis spectra of 5Mn_5.
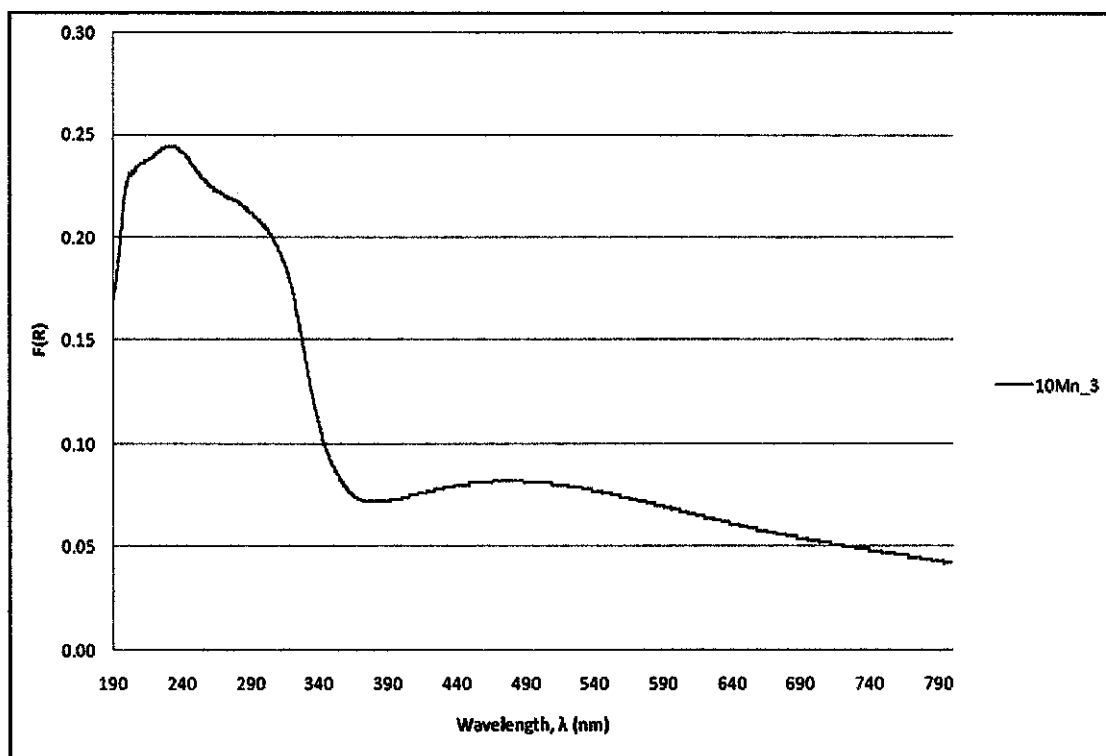
Figure B.7: DR-UV-Vis spectra of 10Mn_3.
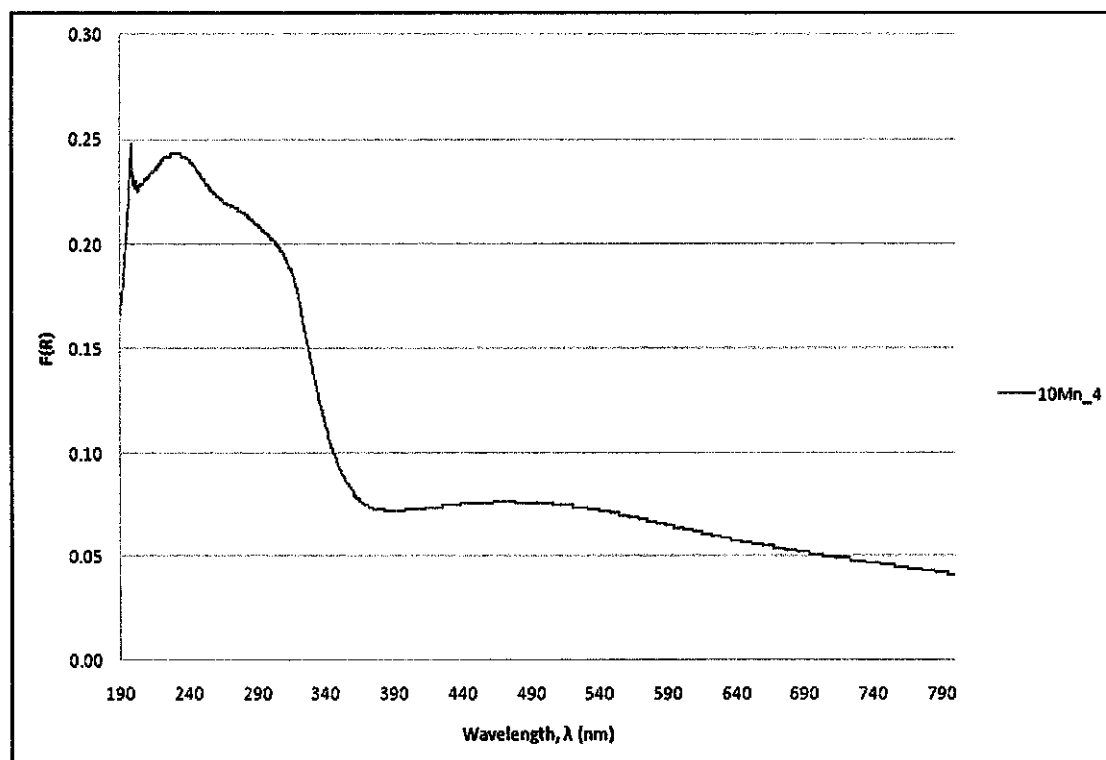
Figure B.8: DR-UV-Vis spectra of 10Mn_4.
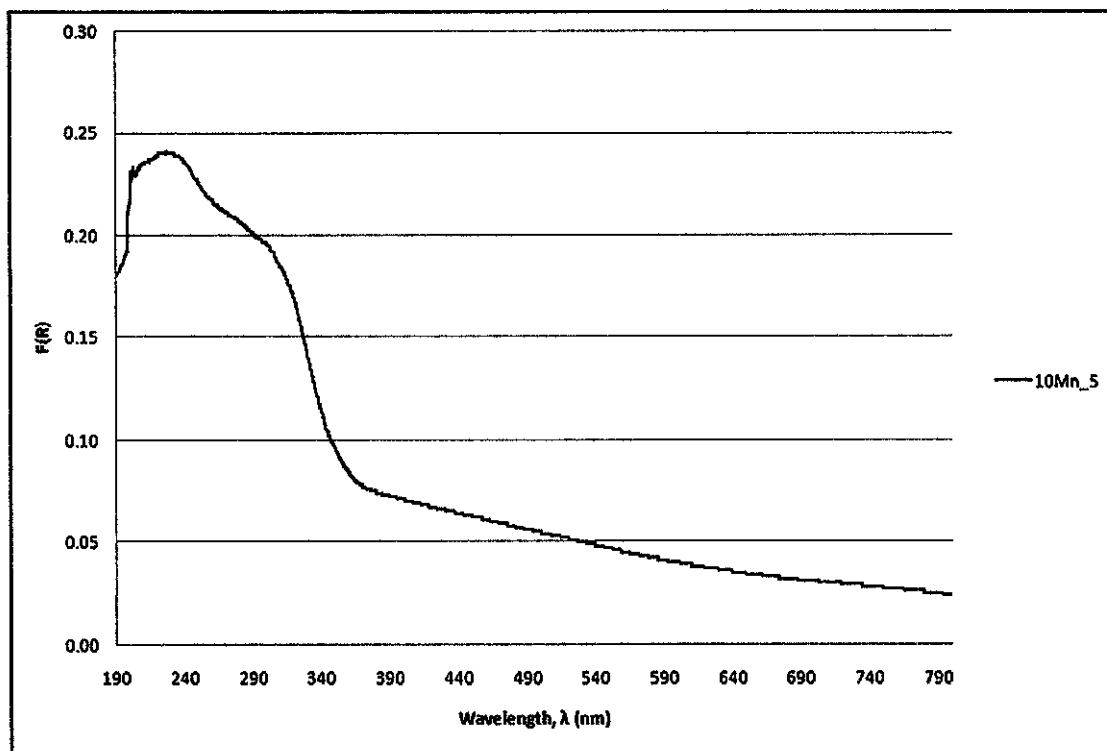
Figure B.9: DR-UV-Vis spectra of 10Mn_5.
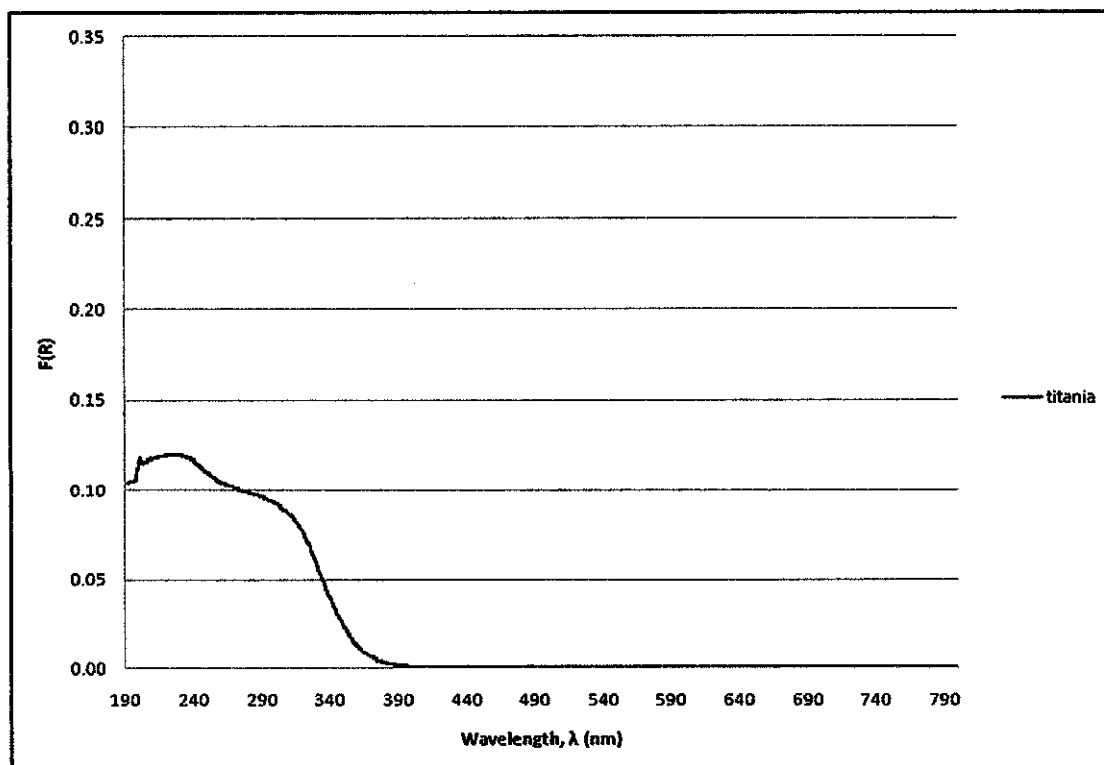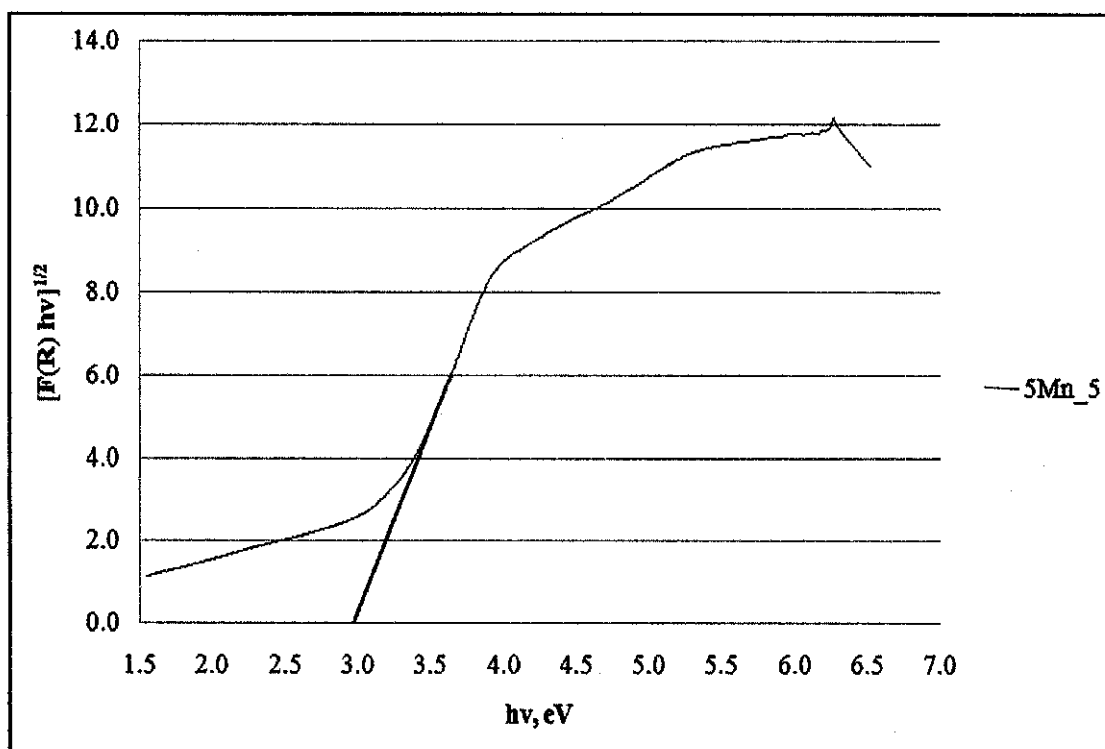

Figure B.10: DR-UV-Vis spectra of titania.

41
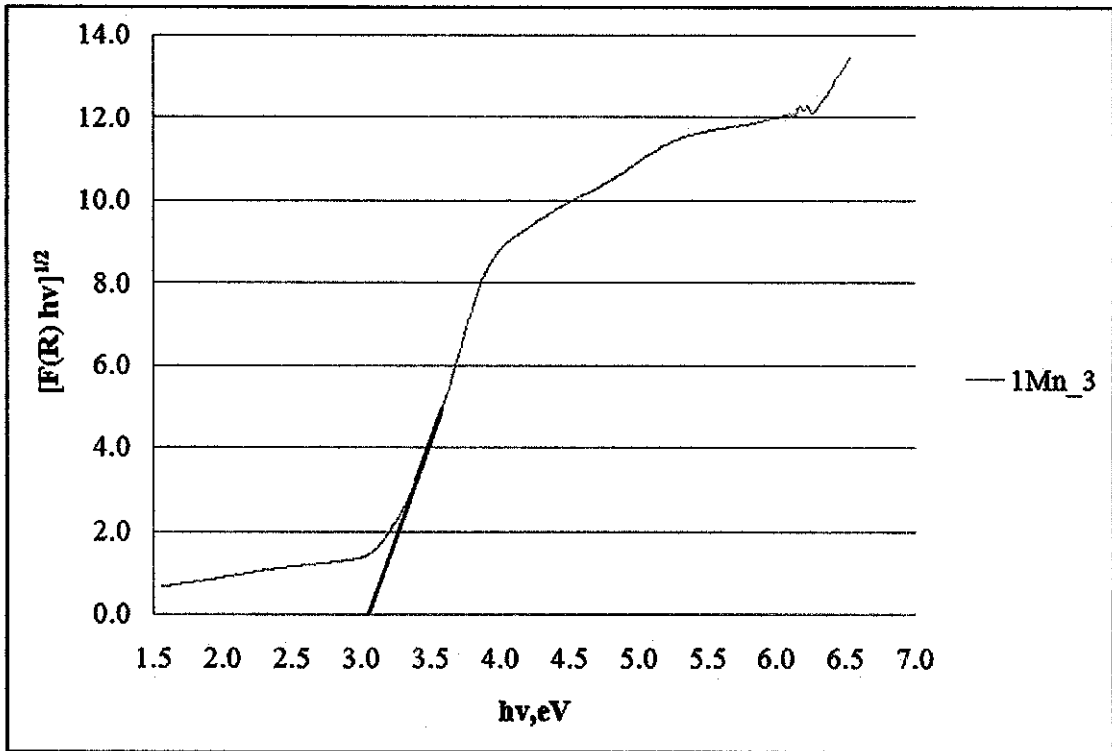
Figure B.11: Plot of transformed Kubelka–Munk functions [F(R).hv]1/2 versus hv for 1Mn_3 to estimate band gap energies by linear extrapolation.
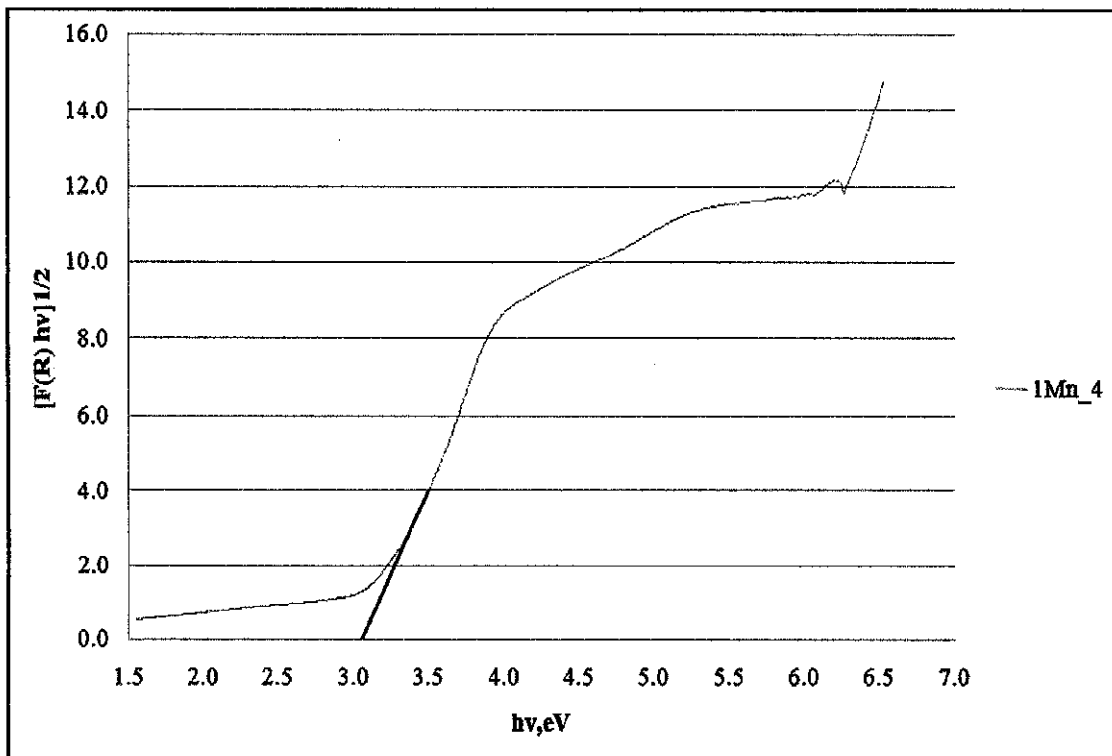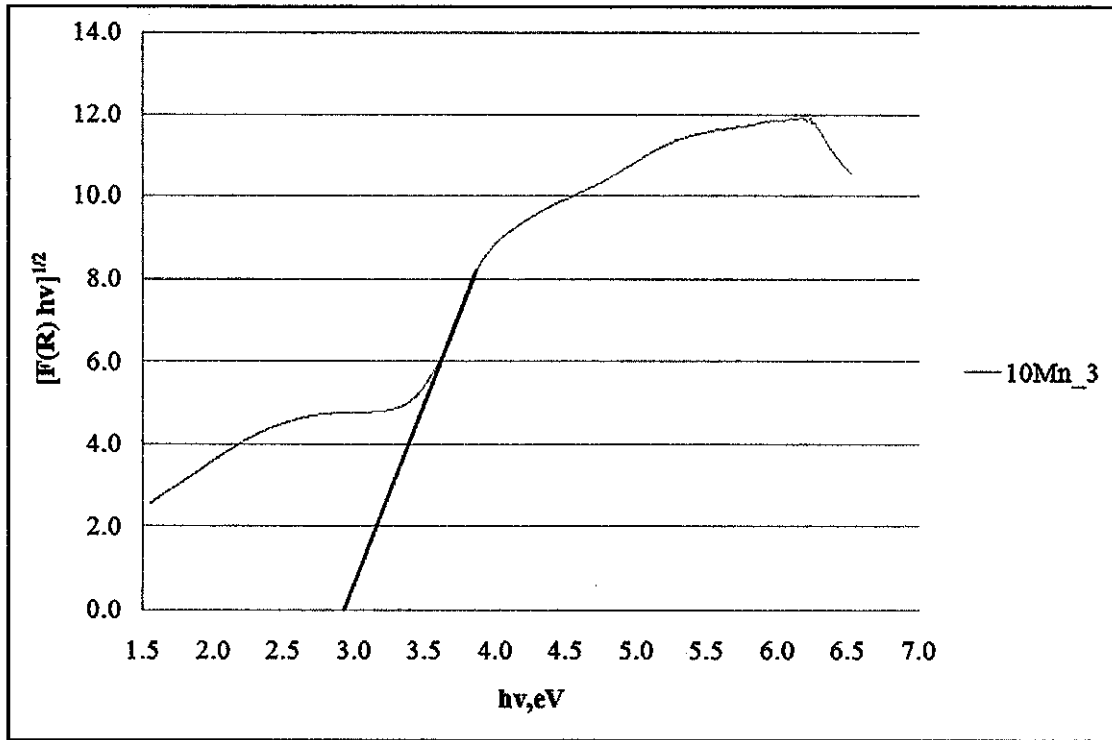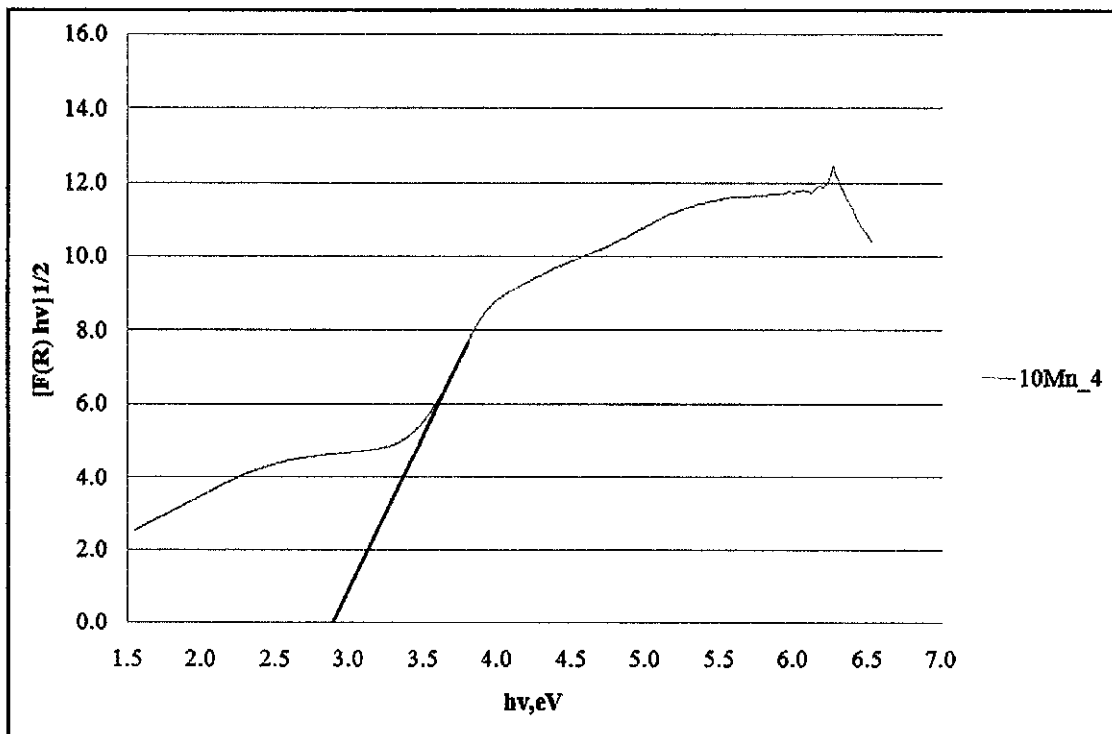

Figure B.12: Plot of transformed Kubelka–Munk functions [F(R).hv]1/2 versus hv for 1Mn_4 to estimate band gap energies by linear extrapolation.
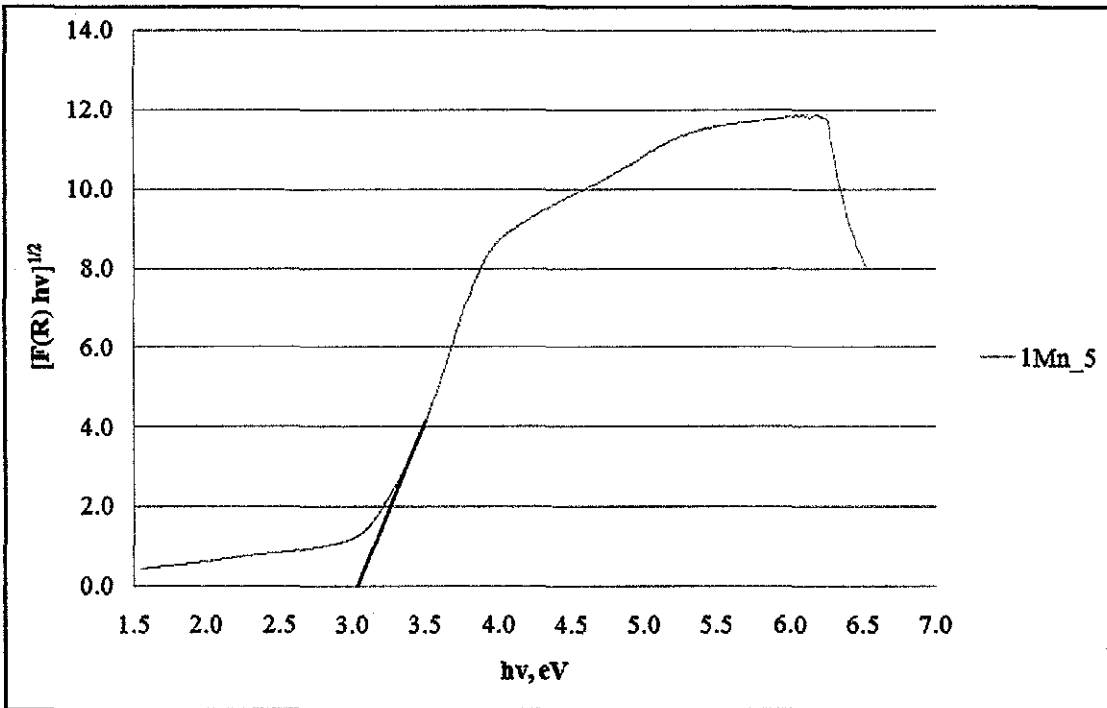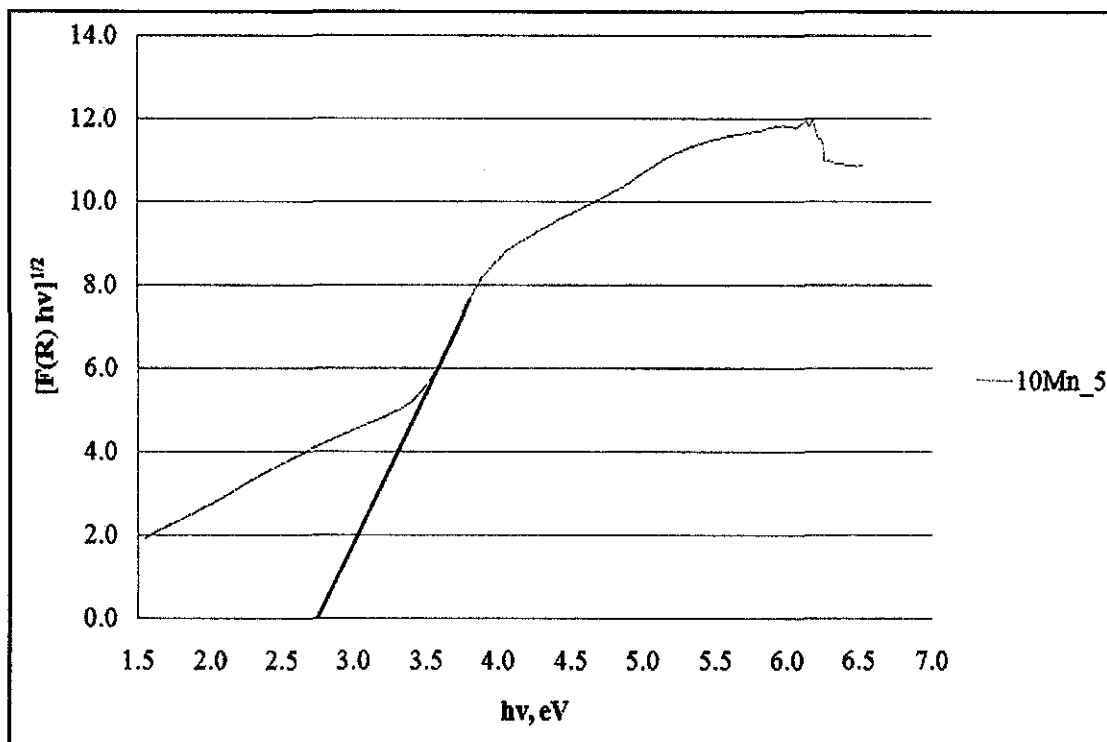
Figure B.13: Plot of transformed Kubelka–Munk functions [F(R).hv]1/2 versus hv for 1Mn_5 to estimate band gap energies by linear extrapolation.
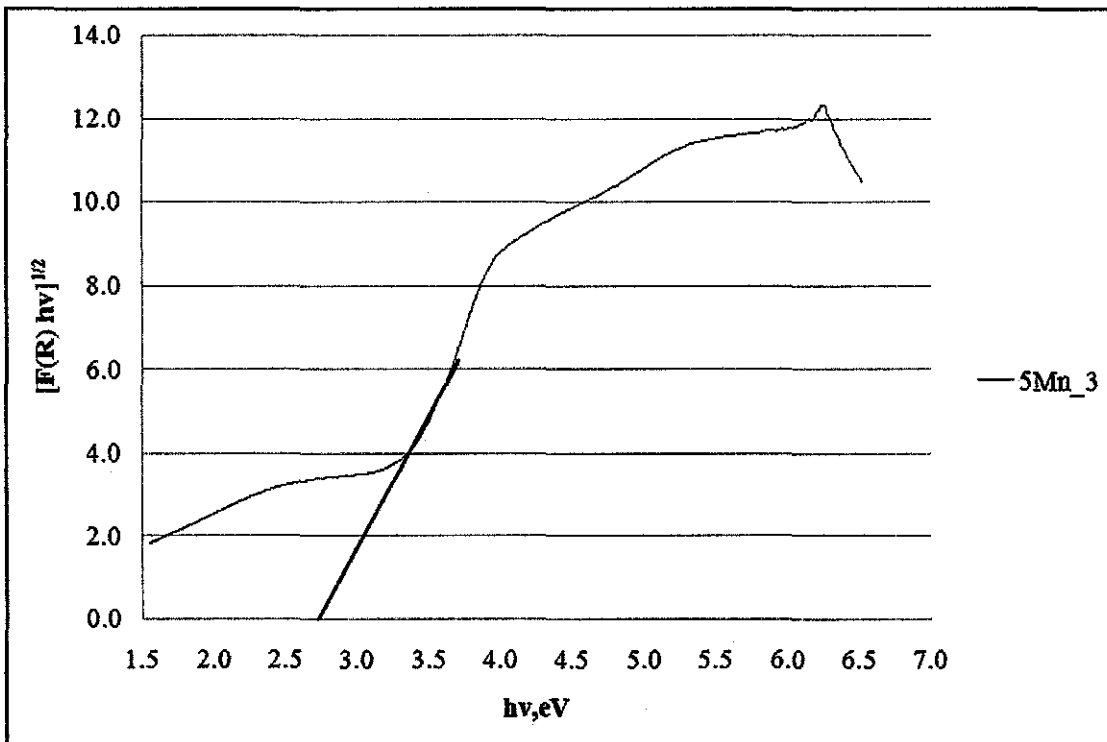
Figure B.14: Plot of transformed Kubelka–Munk functions [F(R).hv]1/2 versus hv for 5Mn_3 to estimate band gap energies by linear extrapolation.
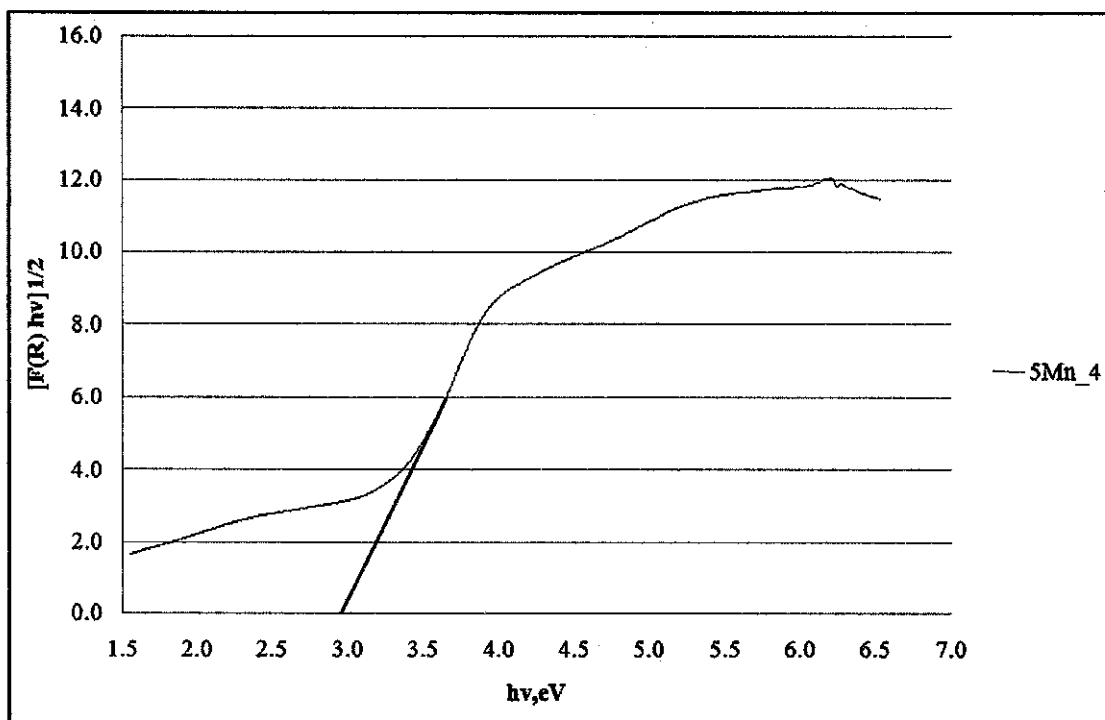
Figure B.15: Plot of transformed Kubelka–Munk functions [F(R).hv]1/2 versus hv for 5Mn_4 to estimate band gap energies by linear extrapolation.

Figure B.16: Plot of transformed Kubelka–Munk functions [F(R).hv]1/2 versus hv for 5Mn_5 to estimate band gap energies by linear extrapolation.
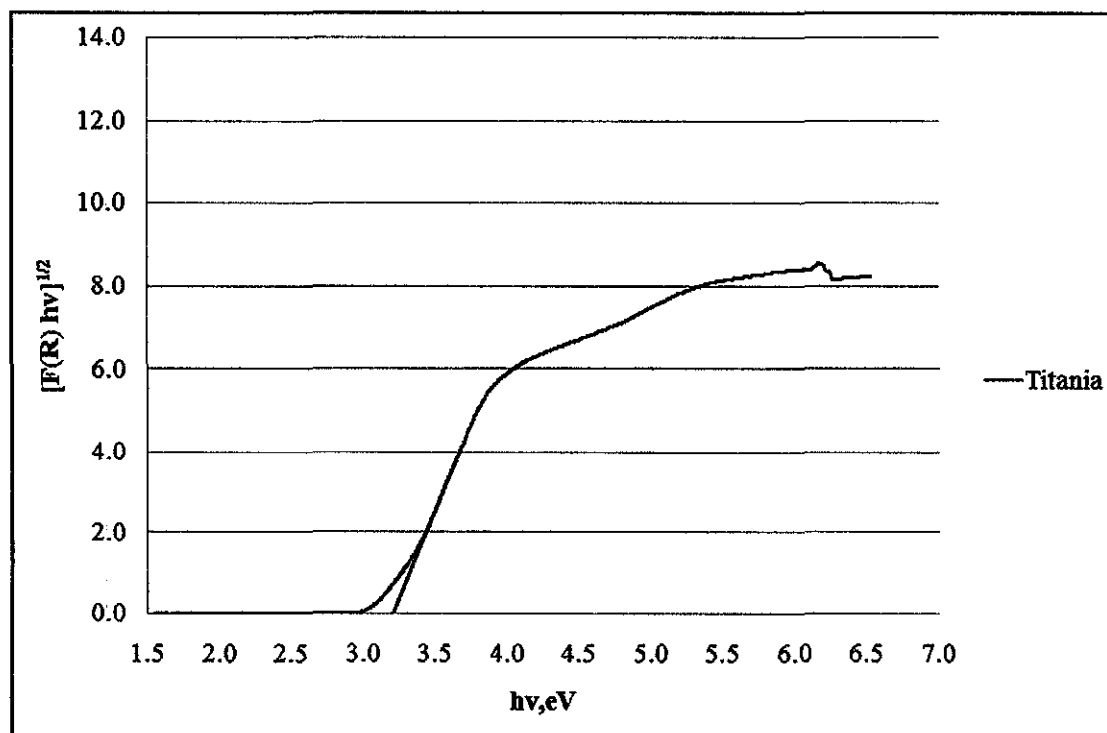
Figure B. 17: Plot of transformed Kubelka–Munk functions [F(R).hv]1/2 versus hv for 10Mn_3 to estimate band gap energies by linear extrapolation.

Figure B.18: Plot of transformed Kubelka–Munk functions [F(R).hv]1/2 versus hv for 10Mn_4 to estimate band gap energies by linear extrapolation.

Figure B.19: Plot of transformed Kubelka–Munk functions [F(R).hv]1/2 versus hv for 10Mn_5 to estimate band gap energies by linear extrapolation.

Figure B..20: Plot of transformed Kubelka–Munk functions [F(R).hv]1/2 versus hv for titania to estimate band gap energies by linear extrapolation.
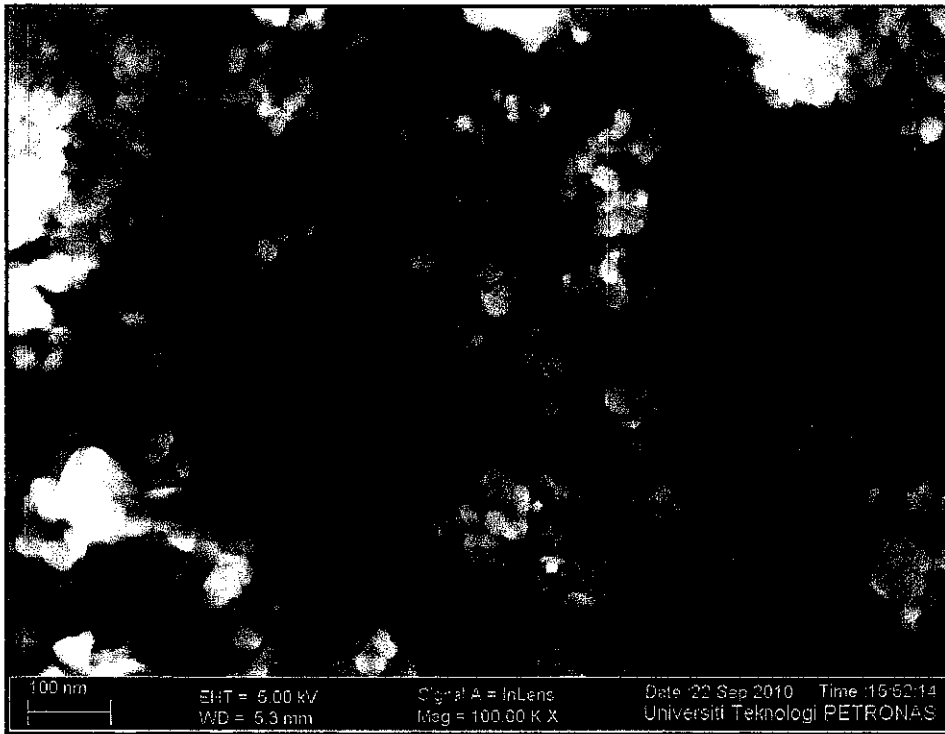
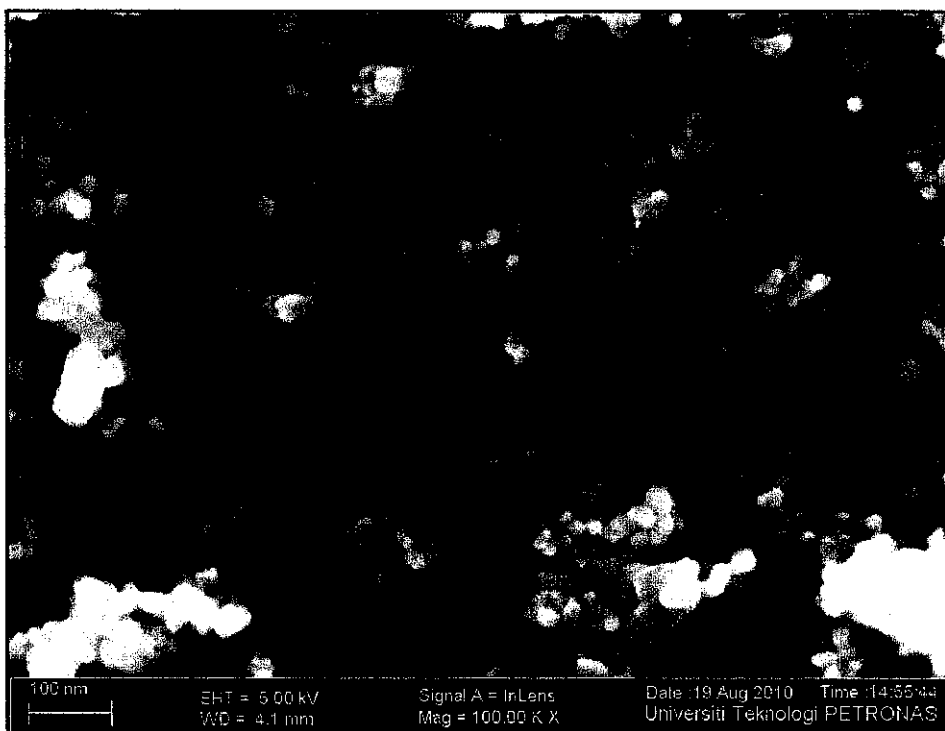**Figure C.1: FESEM micrographs of the 1Mn_3 photocatalyst.**

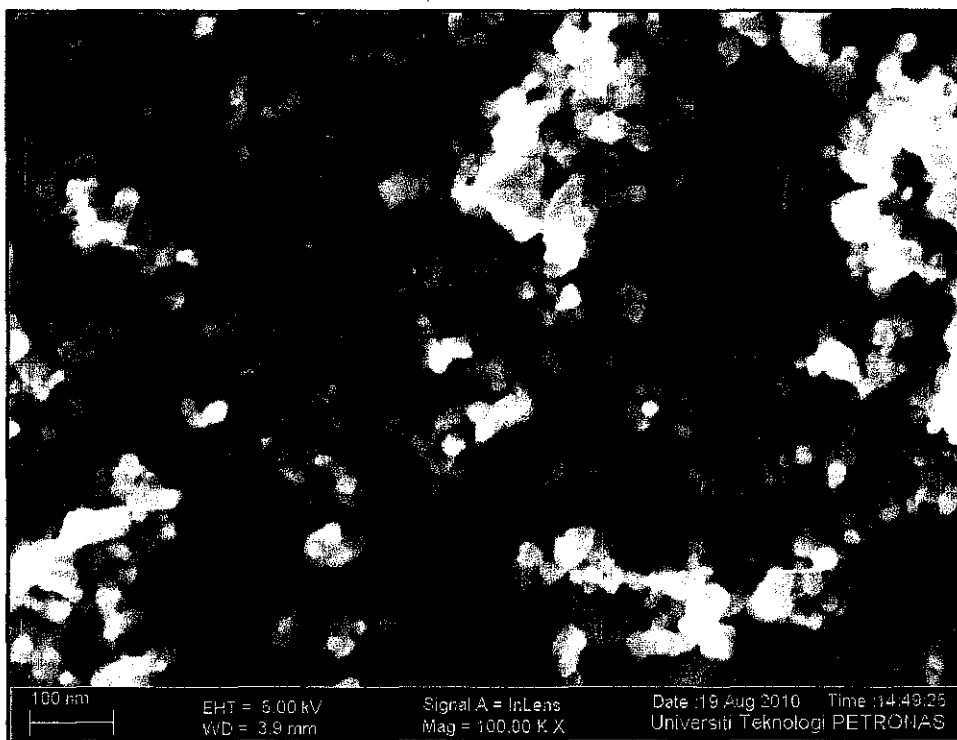**Figure C21: FESEM micrographs of the 10Mn_3 photocatalyst**

Figure C.3: FESEM micrographs of the 1Mn_4 photocatalyst.
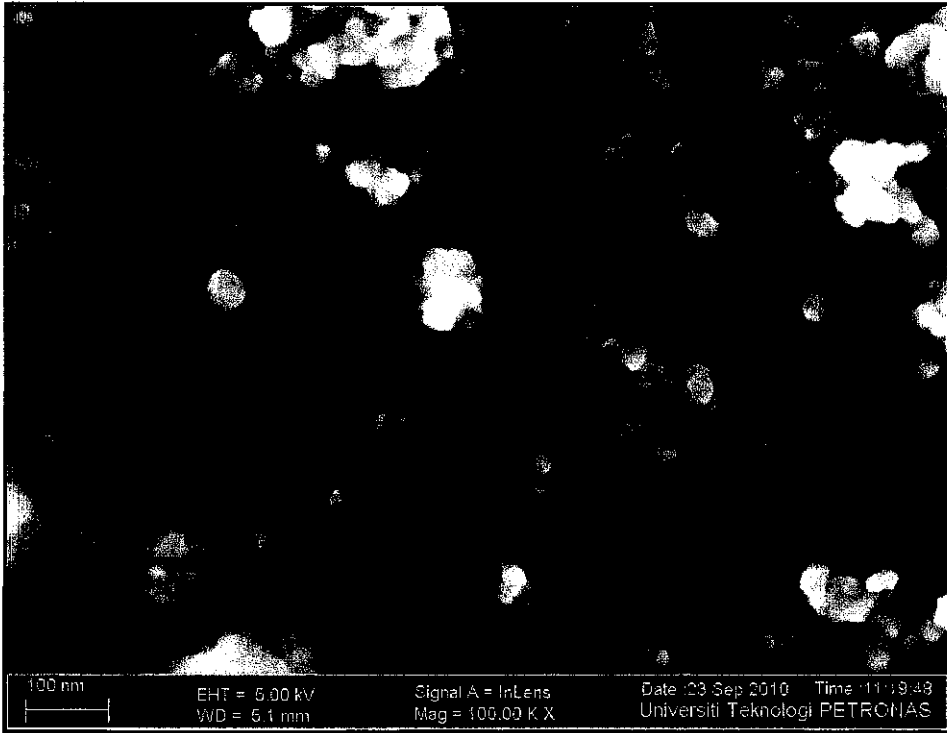

Figure C.4: FESEM micrographs of the 10Mn_4 photocatalyst.

Figure C.5: FESEM micrographs of the 10Mn_5 photocatalyst.